



# Fuzzy logic based adaptive vibration control system for structures subjected to seismic and wind loads

Wisam S. Abdulateef<sup>a</sup>, Farzad Hejazi<sup>b,\*</sup>

<sup>a</sup> Department of Civil Engineering, University Putra Malaysia, Malaysia

<sup>b</sup> Faculty of Environment and Technology, The University of The West England, Bristol, United Kingdom

## ARTICLE INFO

### Keywords:

Magnetorheological damper  
Semi-active dampers  
Fuzzy logic  
Vibration control system  
Multi objective optimization  
Multi verse  
Wind load  
Adaptive structures

## ABSTRACT

In this study, an attempt has been made to develop a Fuzzy Logic Multi Verse Optimal Control (FLMVOC) system as a new adaptive real-time vibration control mechanism for structures subjected to seismic excitation and wind load by utilizing the capability of the stochastic optimization method and fuzzy logic technique.

The magnetorheological damper (MR) is deployed as a controllable vibration damping system in this study due to its excellent damping performance and low energy consumption. Therefore, the analytical model for the MR damper is formulated and integrated with the developed fuzzy logic optimal control (FLOC) algorithm. The story drift and absolute acceleration have been defined as the inputs of the fuzzy logic controller (FLC), while the MR commanding voltage is considered as the controller's output. Then, the membership functions and fuzzy rule base have been formulated. To derive the optimal controller, the FLC with full parameters has been trained with multi objective multi verse algorithm (MOMVO). For this purpose, the MATLAB program and its Simulinks have been integrated and hybridised with finite element package to simulate and evaluate structure response for various input parameters.

The developed FLMVOC system has been implemented in three story shear building subjected to seismic load and 60 story wind induced high rise building in order to evaluate its efficiency in diminishing the dynamic response of the structure.

The result revealed that FLMVOC system successfully reduced structural drifts by 60%, 53%, and 41% under the effect of El Centro, Kobe, and Northridge earthquakes, respectively, while the floor absolute acceleration was reduced by 38%, 17%, and 10%, respectively. For the wind induced structure, the proposed system showed the ability to maintain the floor acceleration within people's comfort criterion in addition to the reduction in story drift.

## 1. Introduction

Recently, researchers and engineers showed enthusiasm and interest in employing semi-active damper systems to mitigate the vibration of structures subjected to external excitation such as seismic and wind load due to their effective performance. Environmental loads on structures and high-rise buildings are the most critical problems for structural engineers since they affect human life and comfort criteria. In contrast to active control, semi-active control device cannot add energy to the controlled structure; instead, its properties can be changed to optimally mitigate structure response to excitation [44]. Furthermore, semi active devices provide the reliability and fail-safe character of passive devices as it does not destabilize the structure (assuming a bound input/bound

output system); also, it possesses the adaptability of active devices. As a result, the focus was shifted to other control systems, particularly semi-active controllers [41].

Magnetorheological (MR) dampers, as one of controllable fluid semi active devices, have been shown as the only reliable intelligent control device in civil engineering applications [8] since they consist of a magnetic based fluid that performs at the same level in a wide range of temperatures (-40° to 150°) and with low commissioning power demand [44,23].

A structure can be defined as adaptive structure when it designed basing on active design paradigm, where the response of the structure is kept within desired values not by over design, instead, it is done by observing unacceptable deviation and compensating it by adaptive

\* Corresponding author.

E-mail address: [farzad.hejazi@uwe.ac.uk](mailto:farzad.hejazi@uwe.ac.uk) (F. Hejazi).

<https://doi.org/10.1016/j.istruc.2023.06.108>

Received 20 January 2023; Received in revised form 20 May 2023; Accepted 22 June 2023

2352-0124/© 2023 The Author(s). Published by Elsevier Ltd on behalf of Institution of Structural Engineers. This is an open access article under the CC BY license (<http://creativecommons.org/licenses/by/4.0/>).

mean in real-time[45].

The adaptive and intelligent real-time structural control mechanism is considered the most critical and demanding component affecting the dynamic response and stability of the structures under applied unsteady loads [57]. The main elements in any adaptive vibration control system consist of; force generation or energy dissipation devices; real-time processing controllers, and sensors, all are integrated with each other within the structure to enhance the structural properties in responding to dynamic loads [42].

Control algorithms, which commands the control device, are the most challenging aspect in active/semi active control systems, hence, it had been attracted the attention of researchers during the past twenty years Jiang et al. [26],Joghataie et al. [27]. Adeli and Kim [1] presented the wavelet-hybrid feedback least mean square algorithm to filter out high frequencies of environmental load subjected to structures and increase the performance of feedback controllers. It is concluded that the proposed control mode can be used to enhance the performance of existing feedback control algorithm. Bel Hadj Ali and Smith Ali et al. [9] presented the vibration control of a five-module active tensegrity structure as a multi-objective optimization problem. The control commands are identified using stochastic search through Probabilistic Global Search Lausanne (PGSL) and PROMETHEE outranking strategy. The rule of the proposed active control system is to attenuate vibrations by shifting values of natural frequencies away from excitation by commanded contracting or elongating the active structs. N. Wang and Adeli [48] developed a self-constructing wavelet neural network algorithm (SCWNN) as an integration of a self-constructing method and the fuzzy compensation controller which it was employed to overcome chattering phenomena in sliding mode control.

Since the centralized control system represents a single point of potential failure Zhang et al. [51], many researchers were shifted to employ the concept of decentralized control system, in which, the structure is decomposed into a substructures with one or more controller, these controllers are rely on local measurements in making control decisions instead of global measurements in centralized systems. Soto et al. [22] utilized decentralized control concept in combining with the concept of replicator dynamics and agent-based modeling of evolutionary game theory to develop multi-agents replicator control methodology (MARC), this methodology was applied on a numerical structures of three story shear building and twenty story shear buildings under the effect of time history and artificial earthquakes. Although, the proposed methodology showed a better performance in comparison with centralized and decentralized LQR control systems, authors mentioned that a very careful consideration should be taken in selecting the parameters of replicator dynamics model. To overcome this limitations, a new version of MARC was presented employing neural dynamic model (NDAP) as a multi objective optimization technique Soto et al. [21].

Despite the existence of various techniques for predicting and quantifying uncertainties in environmental loads, the accuracy of these methods is not always guaranteed, as they can be influenced by factors such as the availability and quality of data and the size of the sample [53]. As one of intelligent controls viable to endure uncertainties and nonlinear behaviour in both environmental loads and structural properties[2], Fuzzy logic controllers (FLC) were utilized by many researchers through unification with other control and optimization methods (especially neuro based FLC) to improve its performance [3,39,32]. Jiang and Adeli Jiang et al. [25] presented a dynamic fuzzy wavelet neuroemulator strategy to predict structure response in advance time steps. The model integrates two intelligent computing (dynamic neural networks and fuzzy logic) and it proposed to use together with a floating-point genetic algorithm to find optimal control force for active systems. In neuro-fuzzy control systems, two approaches are followed, direct and indirect adaptive control scheme, in the former, the dynamics of the system are not known, the controller is directly estimated and the control inputs are generated to insure stability of the system, in the

latter, however, the dynamics of the system are firstly defined then a control inputs are generated according to the certainty equivalence principle [14]. Since the performance of neuro network-based strategies depends on the training data and the effectiveness of the training, Das et al. [16] proposed a new model-free fuzzy logic based control strategy for the MR dampers in framed structures subjected to seismic loads. The proposed strategy doesn't rely on a mathematical model to simulate the control force of MR damper; instead, it employs fuzzy logic inference system by directly fuzzification of the hysteretic relations of MR damper from experimental results to define the fuzzy controller. Kaveh and Khademhosseini [28] employed fuzzy logic inference system to command the optimal voltage for MR damper which was used in conjunction with a Tuned Mass Damper (TMD) system to attenuate vibration in a seismically excited ten story shear building. The fuzzy logic system was used to overcome the complexity evolved in modeling the controlled structure with TMD, the fuzzy rules were optimized by a charged system search (CSS) algorithm, and the results showed a good performance in mitigating the response of the structure. Xu et al., [55] utilized adaptive Fuzzy Logic function to design a proposed Fuzzy Variable Structure Sliding Mode Control (FVFOSMC) algorithm for vibration control of uncertain building structures.

With the development of high strength materials which are being more flexible and lighter in weight, and due to the increasing demand on high rise buildings, recent design trend has been shifted to consider more criteria in addition to strength and serviceability factors, such criteria comprise performance, occupant perception and comfort, reliability and sustainability[24]. Y. Peng and Zhang [38] were addressed the reliability-based design of MR damper in semi active structural control system subjected to stochastic seismic load, they integrated both hrovat algorithm and LQR scheme to trace the optimal active control force, comparative studies were carried out by defining a probabilistic criteria, design scheme and cost function weights configurations. The authors concluded that reliability-based semi active control produced a safer and more reliable structural system than the statistical moments-based semi active optimal control. Zhang et al. (2022) developed a semi-active multiple tuned mass damping system for wind-induced structures by utilizing a displacement reducing bang-bang control algorithm and the mass of the outer double-skin facade (DFS) [56]. However, their approach did not consider the effects of multidimensional and multidirectional wind loads. The nonlinear response of irregular controlled structures with multi tuned mass dampers (MTMDs) was studied by Khazaei et al. [30]. Genetic algorithm (GA) and SAP2000 analysis software were utilized to get the optimal position for TMDs, the results showed that distributed mass dampers were more effective than one point mass in mitigation structural response under nonlinear time history earthquakes.

One approach to decrease the computational demand in the dynamic analysis of symmetric structures with a high degree of freedom is to use a generalized eigenvalue analysis to calculate the structures' natural frequencies and mode shapes employing Group theory [13]. Other example of recent trends of researches in adaptive vibration control systems is the new supervisory adaptive algorithm had been presented by Zafarani and Halabian [50] as a new method to implement the nonlinear structural properties in a semi active control systems for structures with combined translation-torsional response due to structural irregularities. The new methodology is based on the modified clipped optimal model as a model-based control system deployed with MR dampers. The change in structural stiffness during earthquake events traced by utilizing push-over analysis method to get the nonlinear response of uncontrolled structure and save it as off-line data, then these data had been used as supervisory tool to evaluate the structure response at each time step and updating stiffness related values involved in control model. Steffen et al. [54] introduced two new concepts for adaptive structures in high-rise buildings under the effect of static wind load: stress-free adaptations and element moment actuation. These concepts involve the manipulation of the structure's adaptivity through the application of a unit

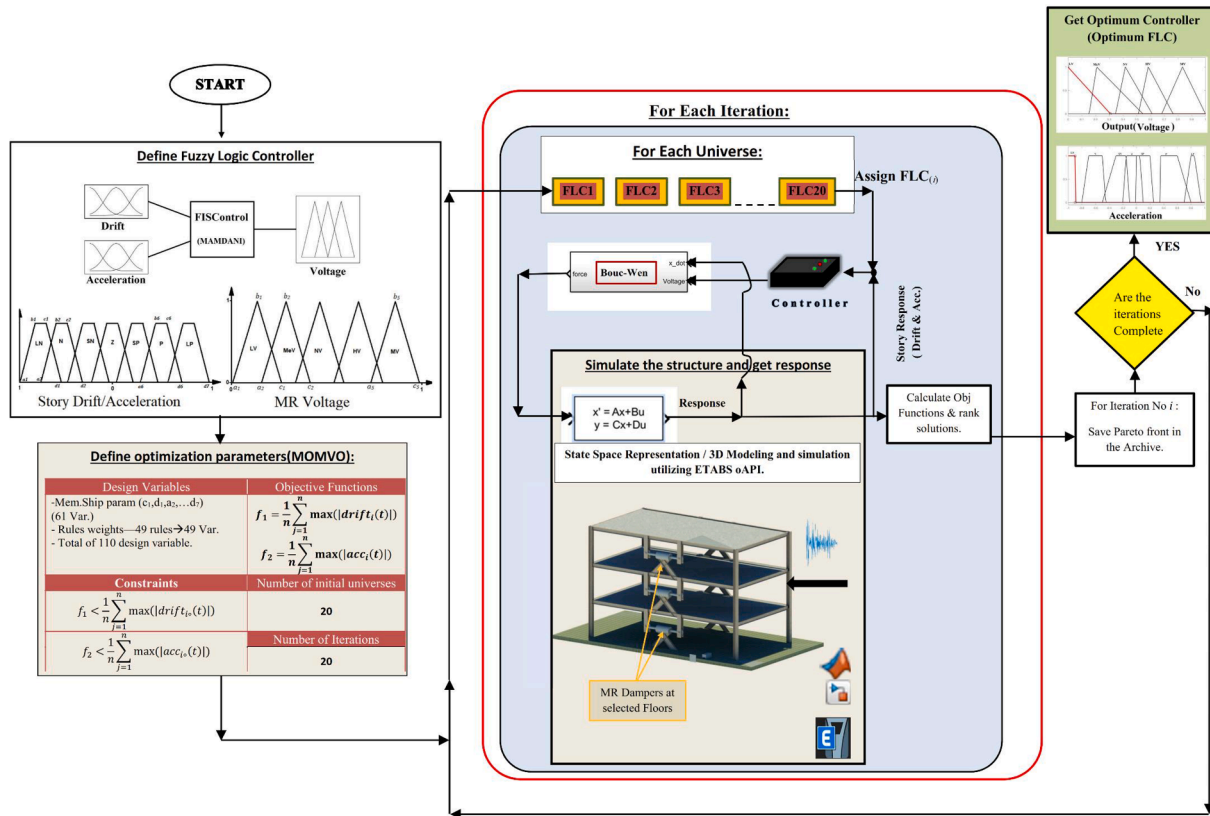


Fig. 1. The flowchart for the developed Realtime Vibration Control Algorithm.

actuation load, followed by the study of the corresponding passive load-bearing behavior. Zhang et al. (2022) utilized the conventional neural network CNN to identify the symmetry group and symmetry order of two-dimensional engineering structures [52]. The supervised deep learning models were adopted. The results showed the efficiency of the developed CNN in identifying the symmetrical properties of the 2D Plans with 86.69% of accuracy. Xu et al. [49] propose closed-form design formulas that consider the nonlinear aeroelastic effect and sensitivity to structural damping in the design of Tuned Mass Damper Inerter TMDI for Vortex-Induced Vibration VIV control of bridges. The formulas provide the required TMDI frequency and damping ratio for a given TMDI mass, inertance, and inerter arrangement to achieve the necessary equivalent damping of TMDI. Wind tunnel experimental data is utilized to validate the proposed formulas. The proposed formulas offer high accuracy and better control efficiency than the existing design formulas for TMDI, which are based on an undamped single-degree-of-freedom primary structure.

It is revealed from critical reviewing of the literature that, the control algorithms play the main role in performance of the structural vibration control systems. The real-time controllers which are continuously evaluating response of structure and commanding on the control devices according to the unpredictable applied dynamic loads to the structures are the most robust way to ensure the system’s reliability to withstand against uncertainties in external excitation and structural response.

Therefore, in this paper, a new fuzzy logic-based real-time vibration control algorithm is developed as a model-free vibration control algorithm for structures subjected to wind and seismic excitations. The full control parameters are derived by off-line training through utilizing multi objective multi verse optimization algorithm. To assess the developed FLMVOC system, it is applied to a three-story shear building subjected to different seismic load records, then the robustness of the controller is examined by implementing it in a wind-induced vibration control system of high-rise building. The contributions of this paper are

as follow:

1. A new Fuzzy Logic Multi Verse Optimal Control (FLMVOC) system is developed as model-free control system which address the limitations of model-based controllers.
2. The developed system revealed a good robustness against uncertain environmental dynamic loads and structural properties, which improves the adaptability of the structural system.
3. The proposed methodology offers a reliable evaluation method that considers the full degree of freedom response in structural analysis.
4. The developed control law can potentially reduce energy consumption and improve the sustainability of the controlled system.

The rest of this paper is organized as follows. In Section 2, the development of the Fuzzy Logic Multi-Verse Optimal Control (FLMVOC) system, along with its related models and assumptions, are demonstrated. Section 3 applies the developed FLMVOC to two structures excited by earthquake and wind loads and assesses its performance. Finally, Section 4 summarizes the main findings of this study and draws conclusion.

## 2. Development of fuzzy logic multi verse optimal control (FLMVOC) system

In this research an attempt has been made to develop a vibration control system based on the fuzzy logic (FL) algorithm, and it utilizes the power of multi verse optimization (MVO) as a powerful stochastic optimization method. The development process for the proposed Fuzzy Logic Multi Verse Optimal Control (FLMVOC) System is summarized through the following steps:

The initial step was development of a Fuzzy Logic controller. In this step, the controller’s inputs, outputs, position of each membership

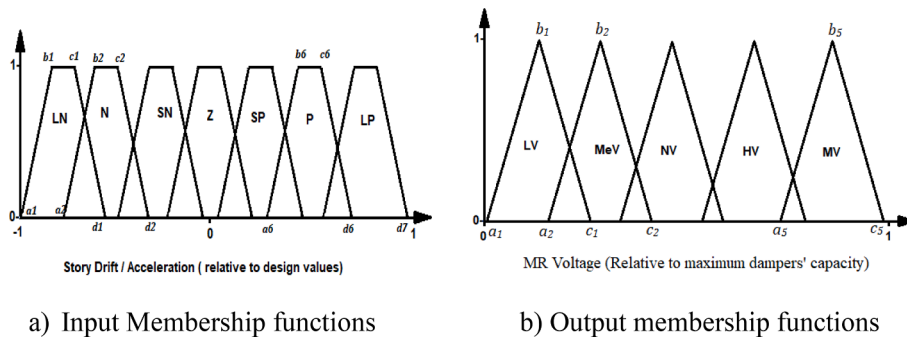


Fig. 2. Proposed Membership Functions For FL Controller.

Table 1  
Proposed FLC Rules For Earthquake Excited Structures.

Acceleration	Drift						
LP	P	SP	Z	SN	N	LN	
LV	MeV	MeV	MV	HV	MV	MV	LN
LV	MeV	MeV	NV	NV	HV	MV	N
LV	LV	LV	MeV	NV	NV	NV	SN
LV	LV	LV	LV	LV	MeV	MeV	Z
NV	NV	MeV	LV	LV	MeV	NV	SP
MV	HV	HV	NV	NV	NV	MeV	P
MV	MV	HV	HV	HV	NV	NV	LP

**Keynote:** LN: Large Negative, N: Negative, SN: Small Negative, Z: Zero, SP: Small Positive, P: Positive, LP: Large Positive, LV: Low Voltage, MeV: Medium Voltage, NV: Neutral Voltage, HV: High Voltage, MV: Maximum Voltage.

Table 2  
Proposed FLC Rules For Wind Excited Structures.

Acceleration	Drift						
LP	P	SP	Z	SN	N	LN	
MV	MV	NV	NV	NV	MV	MV	LN
NV	NV	MeV	MeV	MeV	NV	NV	N
MeV	MeV	LV	LV	LV	MeV	MeV	SN
MeV	LV	LV	LV	LV	LV	MeV	Z
MeV	MeV	LV	LV	LV	MeV	MeV	SP
NV	NV	MeV	MeV	MeV	NV	NV	P
MV	MV	NV	NV	NV	MV	MV	LP

**Keynote:** LN: Large Negative, N: Negative, SN: Small Negative, Z: Zero, SP: Small Positive, P: Positive, LP: Large Positive, LV: Low Voltage, MeV: Medium Voltage, NV: Neutral Voltage, HV: High Voltage, MV: Maximum Voltage.

function, in addition to fuzzy base rule weight are formulated and considered as the optimization’s design variables. The analytical model for Magnetorheological (MR) damper is formulated. The proper platform to model the considered structure is developed.

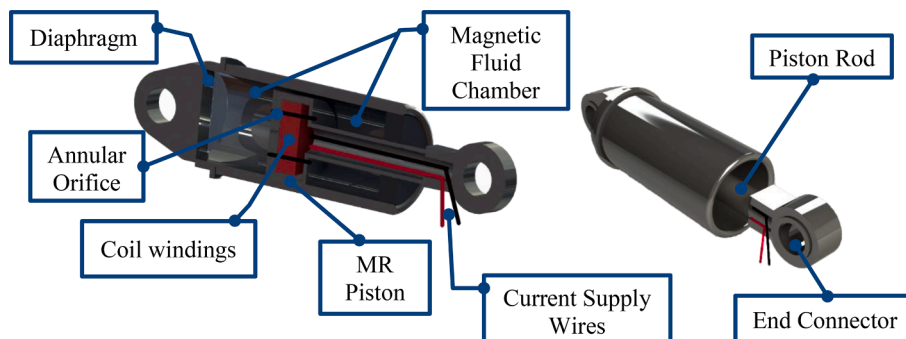


Fig. 3. Schematic View of The MR Damper.

Development of an integrated and synchronized system to connect Matlab software and its Simulink to run optimization process and also real-time controller mechanism to the finite element program such as ETABS program to simulate and analyze the structure under applied load and return the structural response to Matlab for continue optimization and also control process.

All optimization parameters are defined include of optimization’s variables, optimization’s constraints, penalty function, objective function, number of iteration (max time), number of universes (population), maximum archive size, number of objective functions and number of independent iterations.

Define and initiate the optimization process through following steps:

6.1. For each Iteration.

6.1.1. Initialize the universes (each universe represents a fuzzy logic

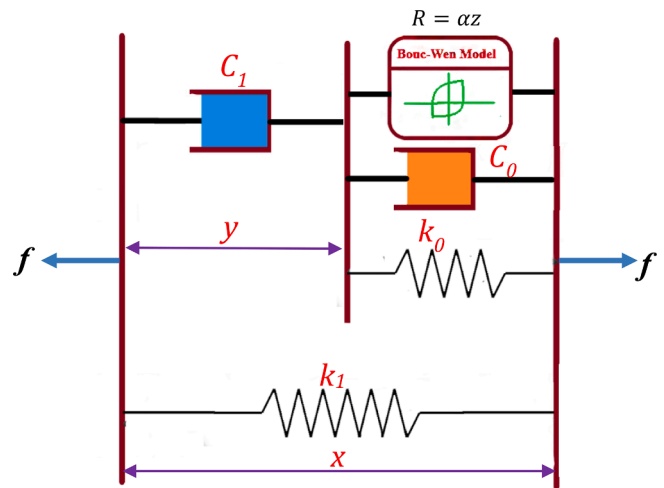


Fig. 4. A Schematic For The Mechanical Model Of MR Damper.

**Table 3**  
Properties of MR Prototype Employed For Earthquake-Excited Problem [19,18].

Physical properties		Electrical Properties	
Stroke Length	±2.5 cm	Peak Power	≤ 10watt
Extended Length	21 cm	Peak Voltage	≤ 3volt
Body Diameter	3.8 cm	Current Driver Type	Linear (Current is proportional to applied voltage)
Fluid Volume	50 ml		
Response Time	10 ms		

**Table 4**  
MR Model Coefficients Used With Earthquake-Excited Structure Aly [4].

Parameter	Value	Parameter	Value
$c_{-a}$	21.0Nscm <sup>-1</sup>	$c_{1a}$	283Nscm <sup>-1</sup>
$c_{-b}$	3.50Nscm <sup>-1</sup> v <sup>-1</sup>	$k_{-}$	46.9Ncm <sup>-1</sup>
$\alpha_a$	140Ncm <sup>-1</sup>	$k_1$	5Ncm <sup>-1</sup>
$\alpha_b$	695Ncm <sup>-1</sup> v <sup>-1</sup>	$x_c$	14.3cm
$c_{1b}$	2.95Nscm <sup>-1</sup> v <sup>-1</sup>	$\gamma$	363cm <sup>-2</sup>
$A$	301	$\beta$	363cm <sup>-2</sup>
$\eta$	190s <sup>-1</sup>	$n$	2

controller).

6.1.1.1. For each universe:

- i) Simulate the structure and apply the time history load.
- ii) Conduct analysis and evaluate the structural response.
- iii) Calculate the objective function.
- iv) Check the constraints and assign penalty function.

6.1.1.2 Save the structural controllers (Universes) in the archive.

6.1.1.3. Rank the solutions (fuzzy logic controllers) according to objective function.

6.1.1.4. Sort and update the archive.

6.1.1.5. Choose the best structural controller (solution), the high ranked solution.

6.2. Start the next iteration.

6.3. When the iterations are completed, select non-dominated structural controllers (solutions) from the archive and put it in pareto front archive, these are called the pareto optimal solutions.

6.4. Run the next independent iteration and repeat the previous steps (6.1–6.3).

6.5. Update the pareto front archive and plot for the pareto optimal solutions.

The optimal Fuzzy Logic controller is selected from pareto optimal solutions, then it is implemented in the vibration control system to command the MR damper.

Fig. 1 shows a flowchart for the proposed optimal control strategy. The above-mentioned steps are demonstrated in details in the following subsections.

2.1. Fuzzy logic controller (FLC)

Fuzzy Logic was presented by Lotfi Zadeh 1965 Vinay et al. [12], it is inspired by how a human making decision when dealing with knowledge that is vague in nature; it is emulate a human expertise in solving problems.

Since the robust systems are defined as ones whose outputs does not change significantly under the influence of input changes, Fuzzy Logic (FL) systems are considered as robust because uncertainties contained in both inputs and outputs are used in formulating the system structure itself[40]. Sometimes it is used to overcome chattering phenomena while maintaining system stability [47]. Nevertheless, it has considered as an example of model-free compensators.

The main contribution of Fuzzy Logic (FL) Systems (or Fuzzy Inference Systems) is that a systematic approach is clearly defined to convert a fuzzy rule base in to nonlinear mapping [31].

**Table 5**  
Bouc-Wen Model's Parameters for Full Scale MR Damper (Aly et al., 2011).

Parameter	Value
$c_{-a}$	4.40Nscm <sup>-1</sup>
$c_{-b}$	44.0Nscm <sup>-1</sup> v <sup>-1</sup>
$\alpha_a$	1.0872e5Ncm <sup>-1</sup>
$\alpha_b$	4.9616e5Ncm <sup>-1</sup> v <sup>-1</sup>
$A$	1.2
$\eta$	50s <sup>-1</sup>
$\gamma$	3cm <sup>-2</sup>
$\beta$	3cm <sup>-2</sup>
$n$	1

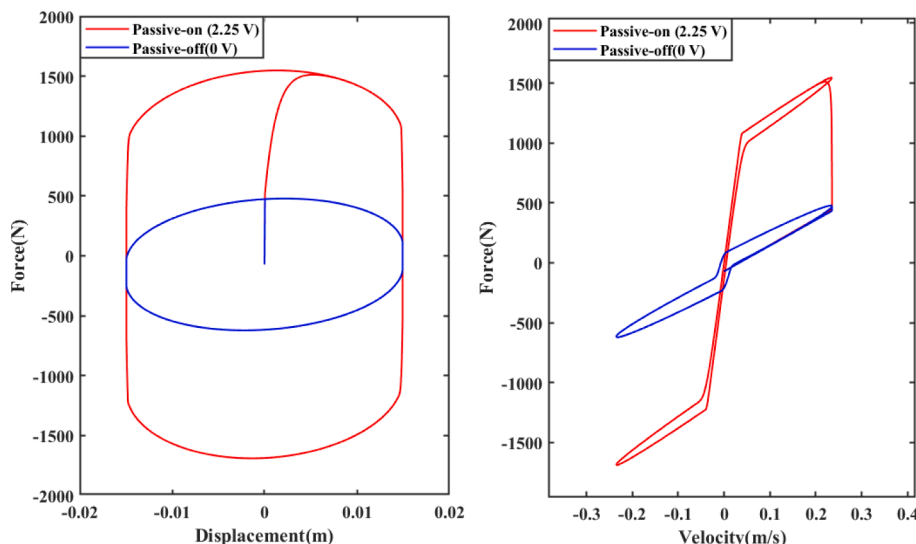


Fig. 5. Simulated Hysteric Curves for the MR model (Force- Displacement and Force -Velocity).

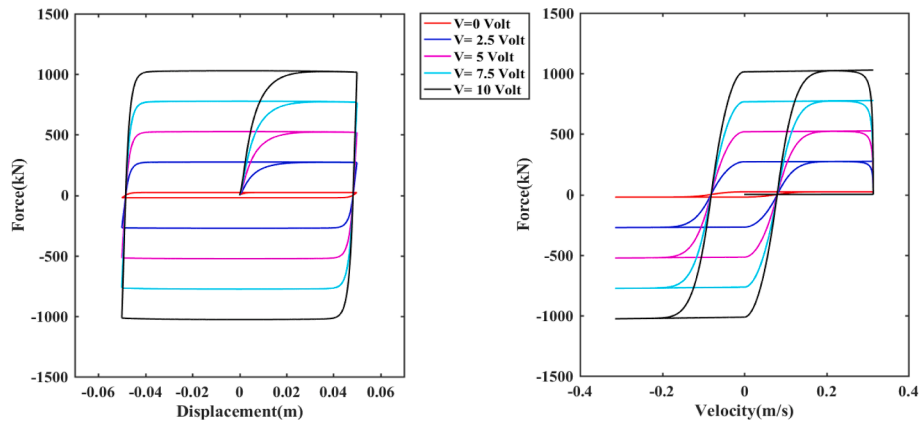


Fig. 6. Hysteretic Curves For the Formulated Mathematical Model of Full Scale MR Damper(1000 kN).

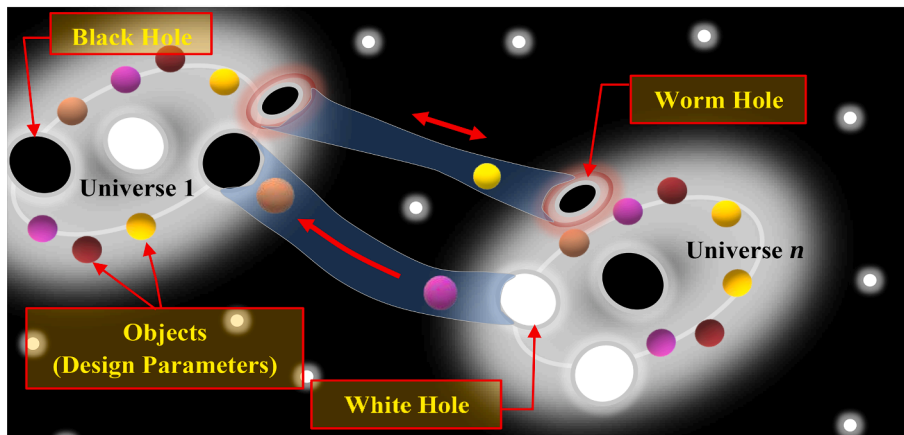


Fig. 7. Demonstration For Multi Verse Theory.

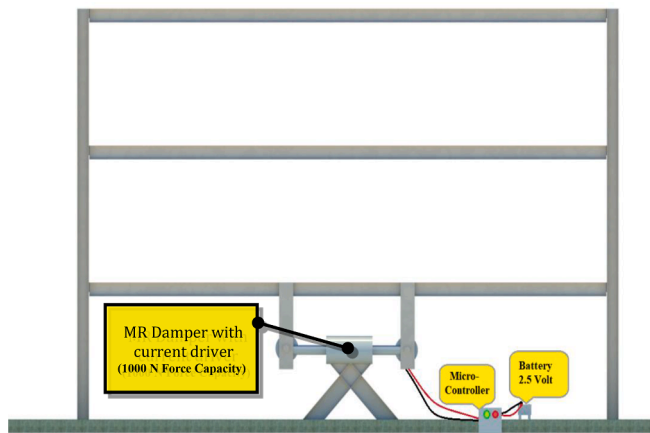


Fig. 8. Schematic For The Scaled Benchmark Structure.

2.1.1. Developing of fuzzy logic controller

In this study, a feedback Fuzzy logic controller is formulated by proposing two inputs: story drift and story absolute acceleration. System output is proposed to be commanding voltage for the MR damper. Membership functions for the inputs were assumed as trapezoidal functions while the output was formulated using triangular membership functions as shown in Fig. 2. Each input has seven shape functions, however, only five membership functions was utilized to define the system output.

Four parameters ( $a_i, b_i, c_i, d_i$ ) per each input membership function must be defined, which are representing the position for each trapezoidal membership function, while only three position parameters should be defined for each output membership function.

It is known that the design of fuzzy logic controller is depending on the designer experience since there is no fixed procedures for it [2]. Therefore, the base rules were proposed according to the expected performance of the MR damper for different load patterns and desired reduction in a specific response. Accordingly, different base rules were proposed to control the structures under the effect of the earthquake and wind excitations. When an earthquake event happens, the desired control action is to reduce story displacement or story drift response. In contrast, controlling the structural acceleration response is more vital when the structure is subjected to the wind load.

The rules are defining the linguistic relationship between inputs and outputs while the rule weights reflect the reliability and allocated contribution of individual rule in the final decision. Table 1 and Table 2 are showing the proposed fuzzy logic controller’s rules, each considered inputs (story drift and story acceleration) are mapped in to seven zones (membership functions) tracing different structural response values, 49 rule are formulated to manage the controller output for different inputs’ cases. For instance, if the story drift is positive (P) value (within excitation direction) and the story absolute acceleration is positive (P), then high voltage (HV) is desired to avoid probability of resonant vibration, in other hand, if the story drift is negative (N) and the acceleration is positive (P), then only a control force within one third of the dampers’ force capacity (Medium Voltage (MeV)) is desired since higher vibration mode are expected. Same logic is employed in formulating the base rules for wind excited structure (Table 2), however, more importance has

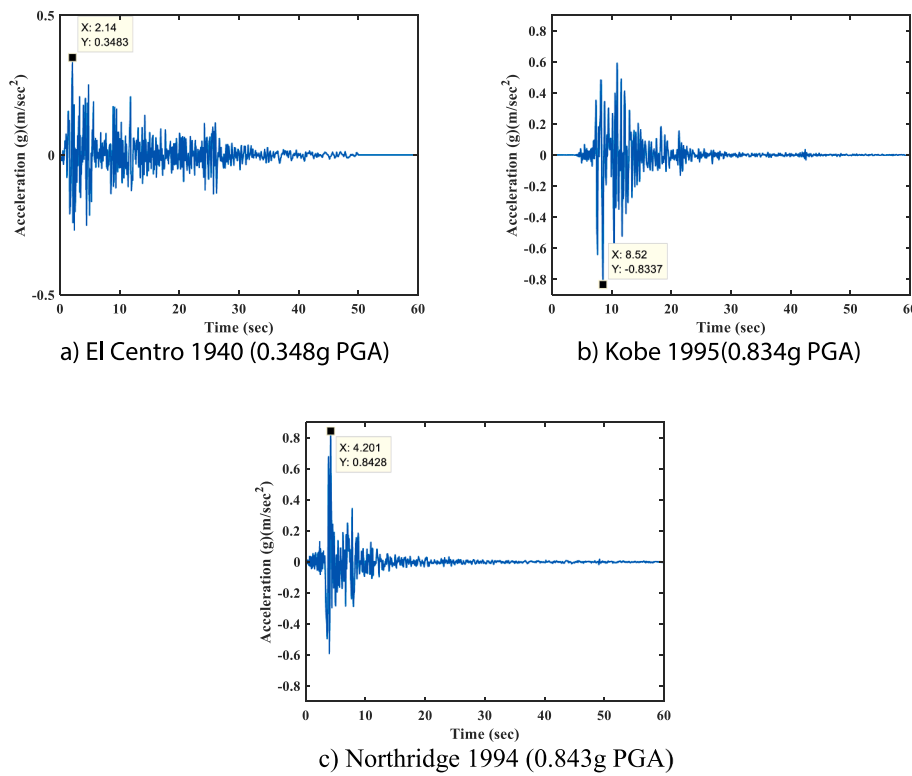


Fig. 9. Historical Earthquake Accelerograms.

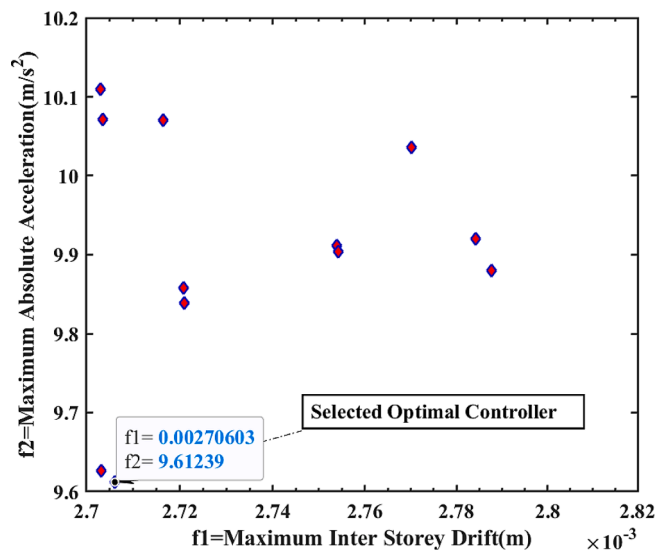


Fig. 10. Pareto Optimal Solutions (Fuzzy Logic Controllers) for Earthquake Excited Structure.

Table 6  
Base rules weights for the optimal Fuzzy Logic controller.

Drift	Acceleration							
	LN	N	SN	Z	SP	P	LP	
LN	MV0.9373	MV0.1615	HV0.0087	MV0.9589	MeV0.9810	MeV0.9810	LV0.6237	
N	MV0.5152	HV0.0027	NV0.7539	NV0.5092	MeV1	MeV0.8117	LV0.5220	
SN	NV0.8128	NV0.4435	NV0.1685	MeV0.1978	LV0.6322	LV0.0038	LV0.7555	
Z	MeV0.6962	MeV0.6840	LV0.0870	LV0	LV0	LV0.9426	LV0.0208	
SP	NV0.2151	MeV0.3215	LV0.3353	LV0.4588	MeV0.7936	NV0.3565	NV0.3510	
P	MeV0.5647	NV0.0495	NV0.7531	NV0.7411	HV0.4303	HV0.0666	MV0	
LP	NV0.8835	NV0.8650	HV0.1518	HV0.4065	HV0.6866	MV0.1245	MV0.6994	

been given to reduce story acceleration. Therefore, despite the high value of story drift (Large Negative, LN, or Large Positive, LP), the desired output voltage is formulated to be within three fifth of the damper capacity (Neutral Voltage NV) when the acceleration is within zero zone (Z membership function) to avoid the probability of increasing acceleration response by applying high magnitude of control force.

Mamdani-type fuzzy inference system has been adopted, here, (MAX) operator is used in fuzzification step, while the truncate (AND) method has been employed in implication step.

The crisp values of inputs are generalized in a closed interval  $[-1,1]$  by dividing measured response by a predefined design values (i.e.,

Table 7  
Optimization parameters for the control system subjected to seismic load.

Parameter	Value
Number of iterations	20
Number of Universes	20
Archive Size	100
Number of independent iterations	5
Objective functions	2
Number of design variables	110

**Table 8**  
Maximum floors' response compared with reference control strategies.

Earthquake	El Centro 1940↓			Kobe			Northridge		
	Story Drift (m)*	Story Acce. (m/s <sup>2</sup> )	Control Force (N)	Story Drift (m)	Story Acce. (m/s <sup>2</sup> )	Control Force (N)	Story Drift (m)	Story Acce. (m/s <sup>2</sup> )	Control Force (N)
Un-Controlled	0.0057	8.5911		0.0102	13.6876		0.0096	13.6775	
	0.0031	10.8437	–	0.0059	18.8327	–	0.0053	17.6166	–
	0.0016	11.3414		0.0032	22.3903		0.0028	19.6229	
FLMVOC	<b>0.0023</b>	<b>5.3258</b>		<b>0.0048</b>	<b>11.3536</b>		<b>0.0057</b>	<b>12.2616</b>	
	<b>0.0017</b>	<b>7.4394</b>	<b>745.6</b>	<b>0.0029</b>	<b>10.3119</b>	<b>714.8</b>	<b>0.0034</b>	<b>11.7932</b>	<b>709.6</b>
	<b>0.0009</b>	<b>6.2903</b>		<b>0.0016</b>	<b>11.4630</b>		<b>0.0018</b>	<b>12.5549</b>	
Modified quasi-Bang-Bang	0.0020	8.0011		0.0051	10.5162		0.0063	13.7783	
	0.0014	5.7418	1106.4	0.0027	10.9882	1155	0.0038	13.5732	1326
	0.0009	5.9307		0.0018	12.7384		0.0022	15.2410	
Clipped Optimal	0.0020	5.2837		0.0043	10.8889		0.0056	11.6457	
	0.0015	5.2530	1108	0.0026	9.5254	1109	0.0032	13.0171	1362
	0.0009	5.9027		0.0014	9.7713		0.0020	13.6943	
Passive On	0.0017	3.5098		0.0043	8.5484		0.0044	9.7169	
	0.0015	4.9965	1108	0.0027	9.3485	1175	0.0034	12.4595	1367
	0.0009	6.0227		0.0014	9.7586		0.0020	13.6095	

\* First row refers to response of first floor.

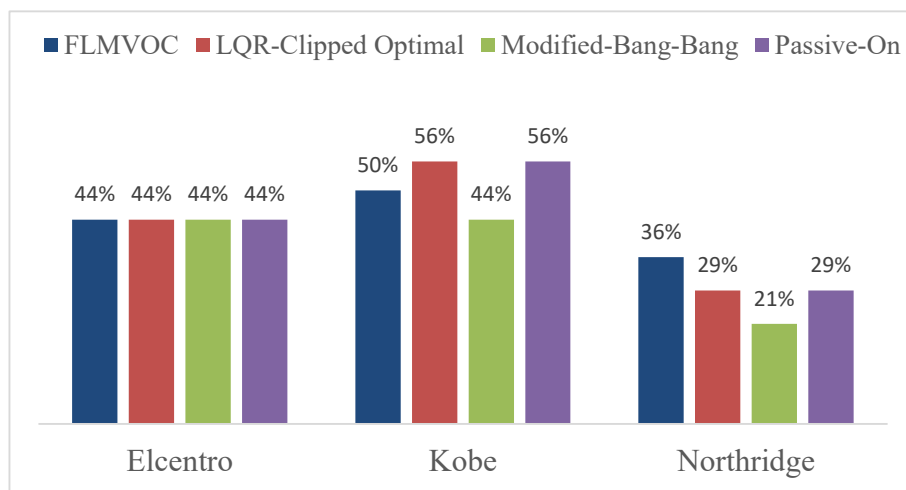


**Fig. 11.** Third Floor Drift Reduction By the Considered Control Strategies.

design drift and acceleration), however, voltage crisp value is defined as generalized value relative to maximum current driver capacity of MR damper, hence it interpreted as [0,1] interval.

Again, the method of MAX (OR) is used for aggregation. While the method of centre of gravity is employed for defuzzification. The FL controller were implemented in proposed control system using MATLAB and FUZZY LOGIC DESIGNER toolbox [33].The graphical form of the proposed membership functions is shown in Fig. 2.

2.2. Magnetorheological damper (MR)

It is proved that semi active control devices are considered as a superior vibration control system in comparison to other types of controllers owing to its efficiency and low power demand. However, MR damper as a semi active device viewed as a kind of prospective device due to its excellent damping performance [38].

To determine the control force generated by MR damper, the mathematical model of Bouc-Wen is utilized to implement MR in the control system.

Although there are many mathematical models were developed by researchers to numerically trace the response of controllable fluid dampers, Bouc-Wen method is the most considered model in the literature due to its very well performance in predicting the control force [37].

In these models, the nonlinearity properties of the damper are modeled by defining differential functions corresponding fluid properties, current, and force each with others. For more details about the development of mathematical models for magnetorheological dampers, the reader can refer to [46]. Fig. 3 shows a schematic view of the MR damper.

2.2.1. The analytical model of MR damper for earthquake excited structure

The modified Bouc-Wen model presented by [44] has been utilized. The force of MR damper is traced by the sum of the forces generated by the original Bouc-Wen model and the nominal damper force due to the accumulator, which is expressed as a fictitious stiffness ( $k_1$ ). To account for the response roll-off of the MR damper when a small velocity is applied, the original Bouc-Wen model was modified to include a dashpot

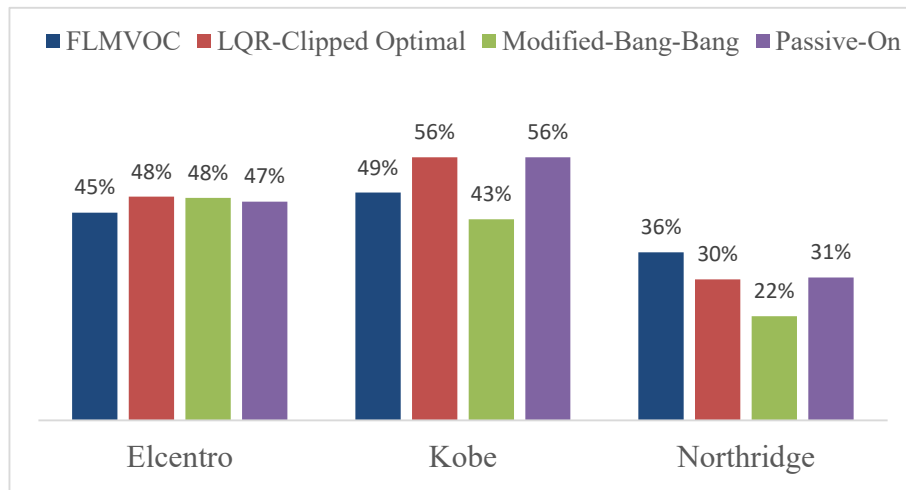


Fig. 12. Third Floor Acceleration Reduction By the Considered Control Strategies.

force ( $c_1\dot{y}$ ) in the force calculation. This modification was necessary to better replicate the phenomena observed in the experimental results [44].

The schematic of the mechanical model of the modified Bouc-Wen model is shown in Fig. 4.

The mathematical expression for the modified Bouc-Wen model is given by the following differential equations [44]:

$$c_1\dot{y} = \alpha z + c_o(\dot{x} - \dot{y}) + k_o(x - y)$$

$$f = \alpha z + c_o(\dot{x} - \dot{y}) + k_o(x - y) + k_1(x - x_o),$$

$$\dot{z} = -\gamma|\dot{x} - \dot{y}|z|z|^{n-1} - \beta(\dot{x} - \dot{y})|z|^n + A(\dot{x} - \dot{y}),$$

$$\dot{y} = \frac{1}{(c_o + c_1)}\{\alpha z + c_o\dot{x} + k_o(x - y)\} \tag{1}$$

Where  $k_1$  is the accumulator stiffness,  $c_o$  is the viscous damping observed at larger velocities,  $c_1$  is the dashpot which is included in the model to introduce the nonlinear roll-off in the force-velocity loops,  $k_o$  is presented to control the stiffness at large velocities, whereas,  $x_o$  is the initial displacement related to the nominal damper force due to the accumulator,  $\gamma, \beta$  and  $A$  are coefficients related to hysteresis behavior of MR damper by which the MR model response can easily be adjusted to represent the actual response accurately.

The MR behaviour under the effect of the magnetic field fluctuating is related to the MR fluid yield stress and the viscous damping constants which found to vary linearly with the change of driving voltage or current Dyke et al. [20,44]. Accordingly, the parameters  $\alpha$ ,  $c_1$  and  $c_o$  are related to the command voltage by the following Eqs. (2) to (4):

$$\alpha = \alpha(u) = \alpha_a + \alpha_b u \tag{2}$$

$$c_1 = c_1(u) = c_{1a} + c_{1b} u \tag{3}$$

$$c_o = c_o(u) = c_{oa} + c_{ob} u \tag{4}$$

$u$  is a parameter reflecting the dynamics involved in the MR fluid reaching the rheological equilibrium and in driving the electromagnet in the MR damper.  $u$  is given by a first order filter expression (Eq. (5)), where  $v$  is the commanded voltage by the current driver,  $\eta$  is a time constant that corresponds to the considered filter.

$$\dot{u} = \eta(u - v) \tag{5}$$

The conventional method to derive above parameters is to run a constraint optimization and simulate the model with optimized values then a comparison between the hysteretic curves for the experimental test and the numerical model must carried out to evaluate the model

[37]. However, for comparison purpose, a predefined parameters in [4] were employed. These parameters had been derived by Dyke et al. [20] for the model of a prototype MR dampers from Lord corporation for testing and evaluation. Table 3 and Table 4 are showing the technical properties for the prototype MR damper and the employed parameters for the analytical model, respectively.

The mathematical model was formulated using MATLAB & SIMULINK Software [33].

To verify the model, a sine wave displacement of 0.015 m amplitude and a frequency of 2.5 Hz is simulated to excite the damper, then the hysteretic curves for the both passive-on and passive-off states were constructed, Fig. 5 shows the hysteretic curves which are observed to match very well to what is presented in literature Aly [4].

### 2.2.2. The analytical model of MR damper for wind-induced structure

Since the considered structure for wind load case is a full-scale structure, the mathematical model of a full-scale MR damper with 1000 kN control force capacity is employed. Following Mousaad et al. [5] and [29], the Bouc-Wen model parameters are utilized and stated in Table 5.

The simplified form of Bouc-Wen model (phenomenological model) is used here, by which, the control force can be predicted accurately Mousaad et al. [5] by the governing differential equations shown below [10]:

$$f = \alpha z + c_o\dot{x} \tag{6}$$

$$\dot{z} = -\gamma|\dot{x}|z|z|^{n-1} - \beta\dot{x}|z|^n + A\dot{x} \tag{7}$$

Same relations in Eqs. (2) to (4) have been employed to implement driver current to the model, moreover, the first filter in Eq. (5) is also utilized here to trace MR dynamics.

To simulate the MR model, aforementioned model has been formulated using MATLAB and SIMULINK, then the hysteretic curves for the MR damper subjected to a sinewave displacement of 5 cm amplitude and 1 Hz frequency for different values of driver voltage ( $V = 0, 2.5, 5, 7.5$  and 10 V) are plotted and compared with reference literature, showing that the model is identical to those used in Mousaad et al. [5] and [29]. Fig. 6 shows the hysteretic curves for the formulated MR damper.

### 2.3. Multi verse optimization (MVO)

Stochastic optimization techniques are the alternative technique to overcome shortcomings of classical approach which it is basing on gradient-decent mathematical method[35].

The multiverse theory is recent and well known in physics[35]. The

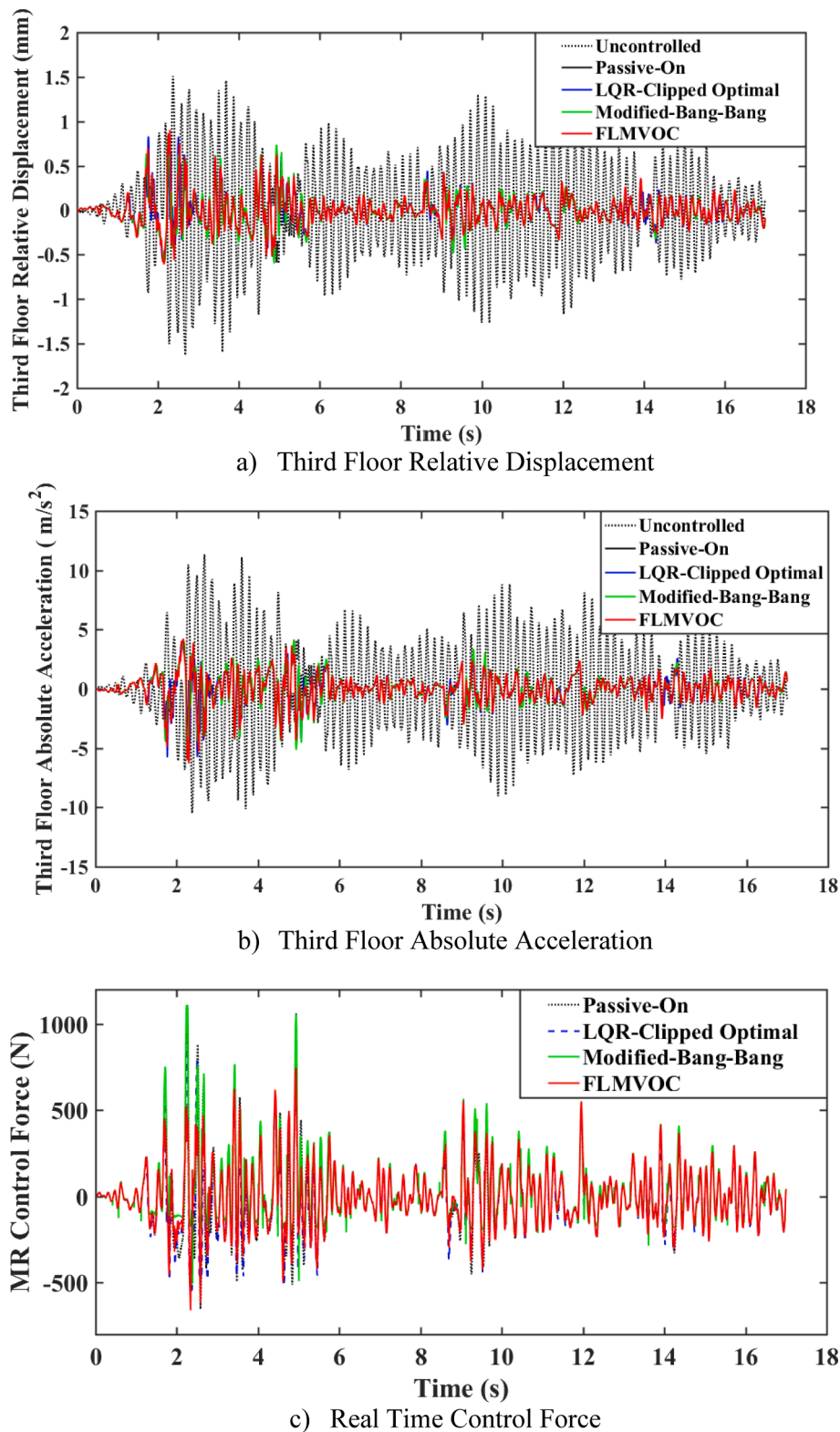


Fig. 13. Comparison of Real Time Structural System Response for the Considered Control Strategy (El Centro Earthquake).

concept behind this theory is that more than one big bang happened; each big bang is responsible for forming a universe. So, there is more than one universe, and the universes exchange objects with each other. Consequently, a different law for each universe is probable.

S.Mirjalili et al. [34] proposed a new multi verse based optimization algorithm (MVO). It is inspired by the interaction of multiple universes via white holes, black holes, and worm holes. According to this theory,

objects are transferred from a universe through a tunnel from a white hole to a black hole. Also, worm holes can transport objects (i.e. design parameters) between universes (solutions) without a need for a white or black hole (Fig. 7). This algorithm can be classified as evolutionary algorithm under stochastic approach of optimization.

The main difference between the Genetic Algorithm (GA) and MVO is that cross over in GA happens for parts of parents and new generation

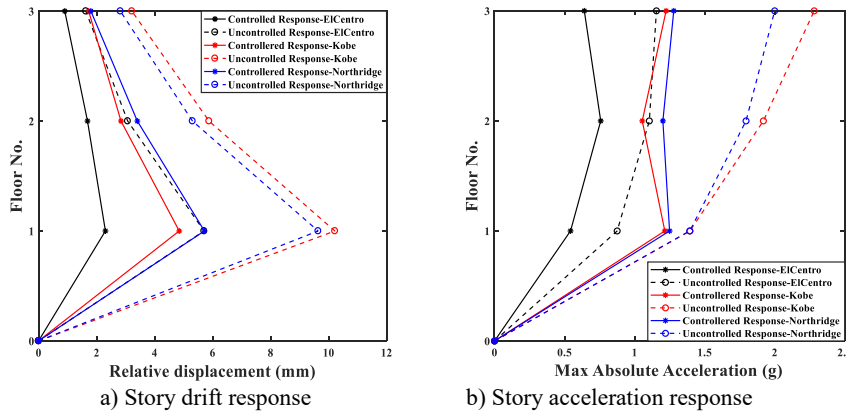


Fig. 14. Maximum Controlled And Uncontrolled Response For The Structure Subjected To Different Earthquakes.

are generated from only two parents of selected parents, while MVO allows any solution to contribute to the creation of new solutions. In addition, MVO has elitism feature and preserve the best solution obtained so far. This means MVO has improved exploration and exploitation mechanism. For insight information, the reader can refer to [35].

In MVO each universe is a solution, and each design variable is an object in the universe, wormholes are considered to ensure exploiting by allowing objects to travel instantly in each universe and even between different universes. For each solution (universe) there is inflation rate (fitness function) assigned to it. Through the optimization process, the iterations are termed as time since it is a common term in multi-verse theory and cosmology.

MVO is running using the following rules:

- The higher inflation rate, the higher probability of having white hole (existence of universe/solution).
- The higher inflation rate, the lower probability of having black holes (lower probability of abrupt changing in variables/objects).
- Universes with higher inflation rate tend to send objects through white holes (travel of good variable's values to the solutions with bad fitness value).
- Universes with lower inflation rate tend to receive more objects through black holes.
- The objects in all universes may face random movement towards the best universe via wormholes regardless of the inflation rate (random improvement in all universes to balance between exploration and exploitation).

2.3.1. Mathematical expression for MVO

In order to mathematically model the concept of objects' exchange between universes, the authors [35] utilized a roulette wheel mechanism, by this mean a random solution (universe) are selected to have a white hole.

The selection process is done after sorting the universes according to its normalized inflation rates, so that, and for minimization problems, the less inflation rate, the higher probability to sending objects through white/black hole tunnels. Although Exploration can be guaranteed using this mechanism, exploitation is not violated because of existence of wormholes in each universe which ensure the transporting of objects between universes randomly without consideration of inflation rates.

Furthermore, the wormholes tunnels are always set up between a universe and the best universe formed so far (universe with high inflation rate), Fig. 7, this is to ensure local changes for each universe and consequently increase the probability of improving its inflation rate.

The mathematical expression for the abovementioned strategy is shown as follows:

$$X_i^j = \begin{cases} \begin{cases} X_j + TDR((ub_j - lb_j)r_4 + lb_j) & r_3 < 0.5 \\ X_j - TDR((ub_j - lb_j)r_4 + lb_j) & r_3 \geq 0.5 \end{cases} & r_2 < WEP \\ X_i^j & r_2 \geq WEP \end{cases} \quad (8)$$

$X_j$  refers to the  $j^{th}$  parameter of the best universe, TDR and WEP are a coefficient,  $ub_j$  and  $lb_j$  are the upper bound and lower bound for the  $j^{th}$  parameter, respectively.  $r_2, r_3, r_4$  are random numbers in [0,1] interval.  $X_i^j$  is the  $j^{th}$  parameter for the  $i^{th}$  universe.

The main two coefficients here are Travelling Distance Ratio (TDR) and Wormhole Existence Probability (WEP), the former is the distance rate to transport objects around the best universe, this value is changes increasingly over the iterations to ensure precise exploitation around the best universe, on the contrary, WEP coefficient is presented to ensure exploration over the advance of optimization process.

Although WEP and TDR can be assumed constants over the optimization process, it recommended to use the following relations to update these coefficients adaptively over the iterations [35]:

$$WEP = min + l \left( \frac{max - min}{L} \right) \quad (9)$$

$$TDR = 1 - \frac{l^p}{L^p} \quad (10)$$

Where (min) is minimum value of WEP, (max) is the maximum value of WEP,  $l$  is the current iteration,  $L$  is the maximum number of iterations.  $p$  is the exploitation/local search accuracy, i.e., the higher  $p$  the higher accuracy of local search.

In this study the values of 0.2, 1, and 6 are used for min, max and  $p$ , respectively.

2.3.2. Multi objective multi verse optimization (MOMVO)

The multi objective version of Multi Verse Optimization algorithm which had been presented by Mirjalili S. et al. [34] was employed in this research. It is basing on the original version of MVO, however, an archive with updating methodology was developed to maintain and improve the coverage of pareto optimal solutions.

In this algorithm, like other population-based stochastic algorithm with multi objective functions, the concept of pareto optimality is utilized, in which the best solution is selected by employing pareto optimal dominance operator to compare different optimal solutions for different objective functions.

The archive technique utilizes storage for pareto optimal solutions obtained so far and improve this set with the progress of optimization. Although the search mechanism is the same in MVO, the best solutions obtained so far (white holes), and the worm tunnels must be chosen from

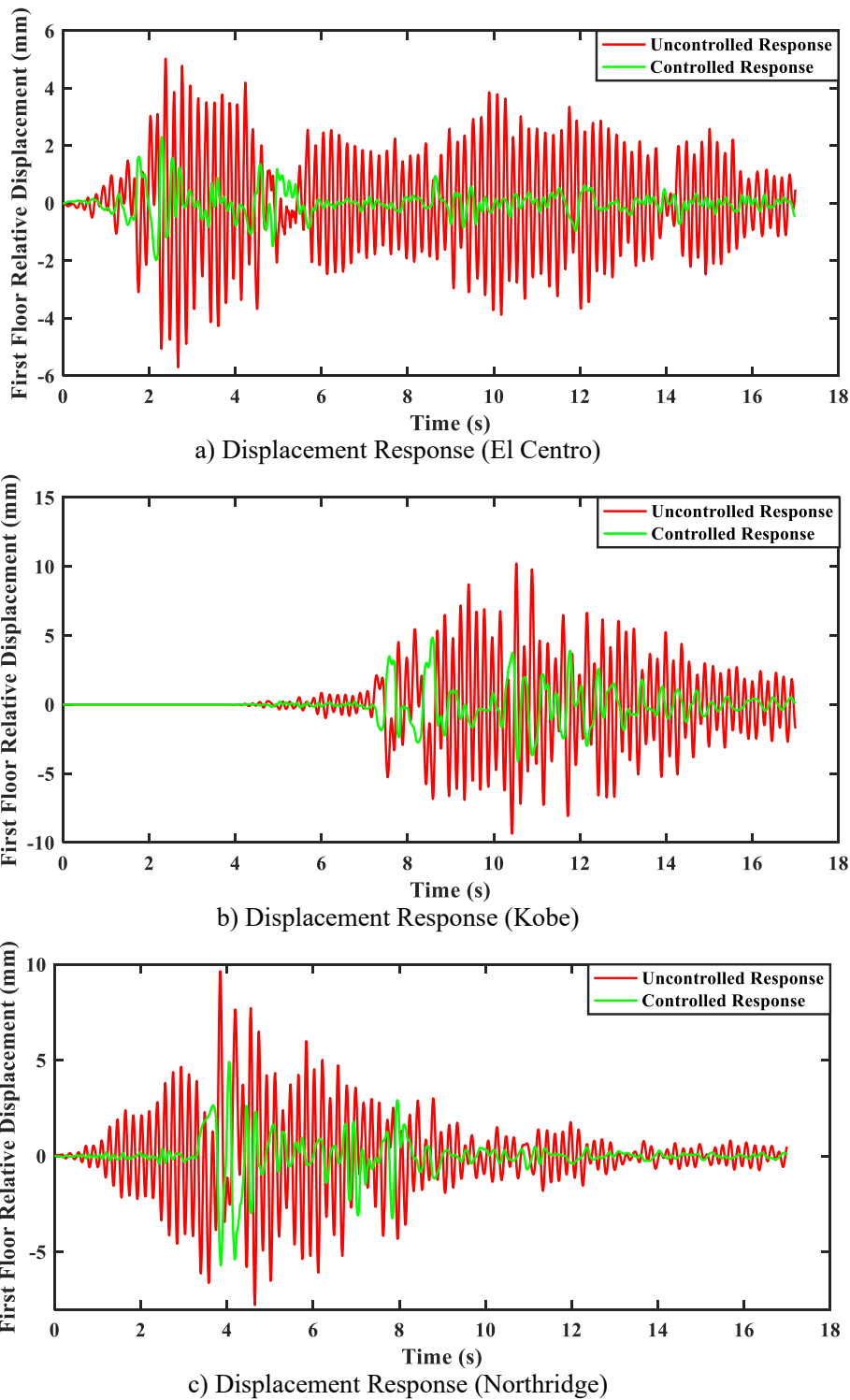


Fig. 15. Realtime Displacement Response For The First Floor Of Strucrure With Optimal FLC (FLMVOC Control Algorithm).

the archive due to the existence of multi non dominated solution for multiple objectives.

To accomplish that, a leader selection mechanism has employed so that the crowding distance between each solution in the archive is firstly selected and the count of neighbourhood solutions are calculated as a measure of converge or diversity.

To improve the distribution of solutions in archive across all objectives, MOMVO employed roulette wheel method to select the best solution from the less populated regions of the archive (solutions with low

inflation rate); the equation used to mathematically express this mechanism is as follows:

$$p_i = \frac{c}{N_i} \tag{11}$$

Where  $c$  is constant and should be more than 1,  $N_i$  is the number of solutions around the  $i^{\text{th}}$  solution. This would improve the probability of the less populated solutions to contribute to the improvement of others.

To guarantee that archive is not getting full during the progress of

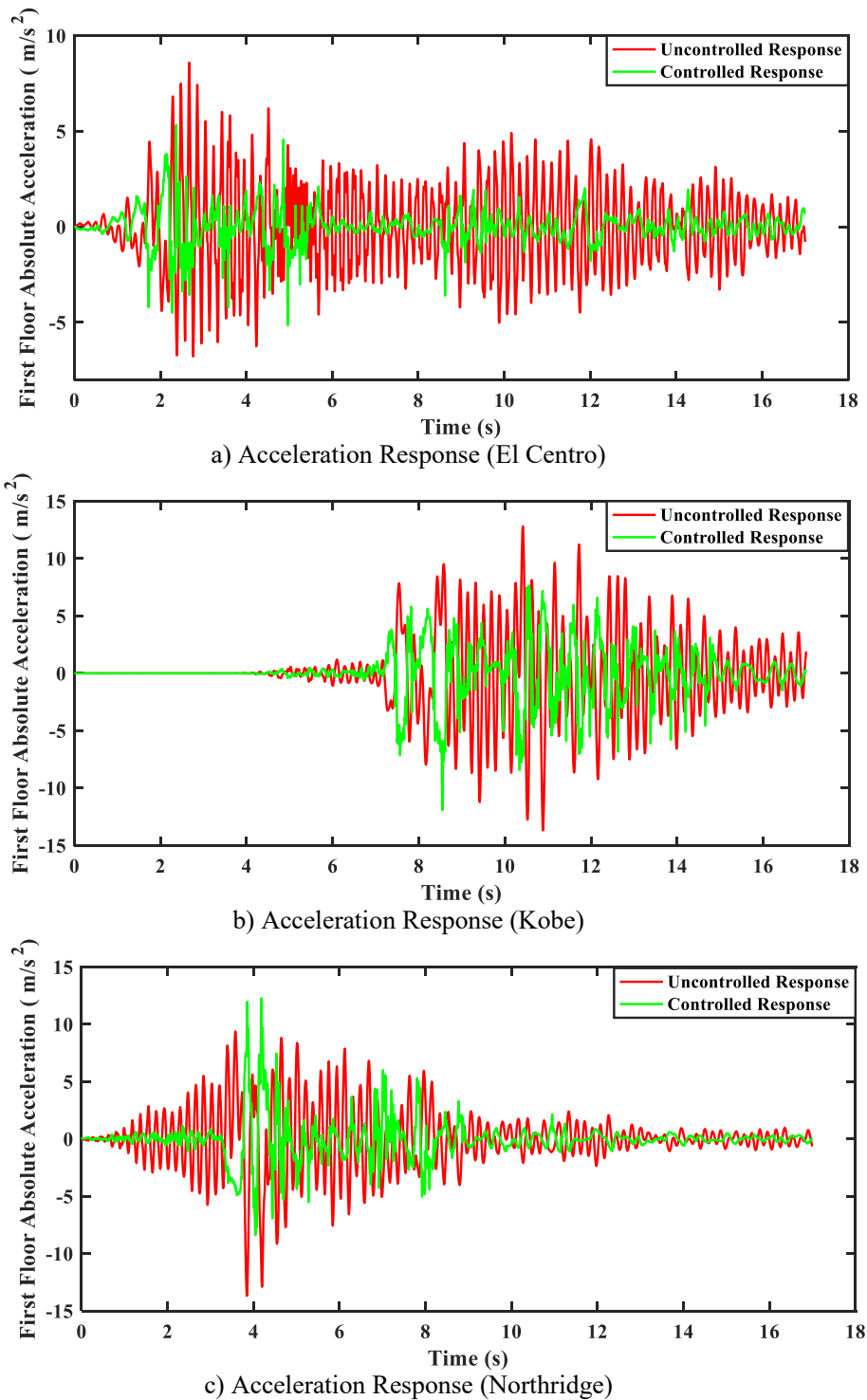


Fig. 16. Realtime Acceleration Response For The First Floor Of Strucrure With Optimal FLC (FLMVOc Control Algorithm).

optimization process, the undesirable solutions; those with many neighbourhood solutions are thrown out of the archive using the inverse of the previous equation. So that:

$$p_i = \frac{N_i}{c} \tag{12}$$

Where  $c$  and  $N_i$  are defined as stated in (11),  $p_i$  is the neighborhood index,  $c$  is maintained as constant with a value more than one, however, in this study, a constant of one was used.

It is found that in case of real structural problem and when two

subsequent solutions are identical (which is highly probable to happen when numerical simulation is used), the archive has been left without any solution, which it leads to cease the optimization process at all. To solve this problem the UpdateArchive function of the source code was modified, and then the optimization algorithm has been tested before applying it in the proposed methodology.

#### 2.4. Objective functions

In this work the superiority of MOMVO algorithm in carrying out

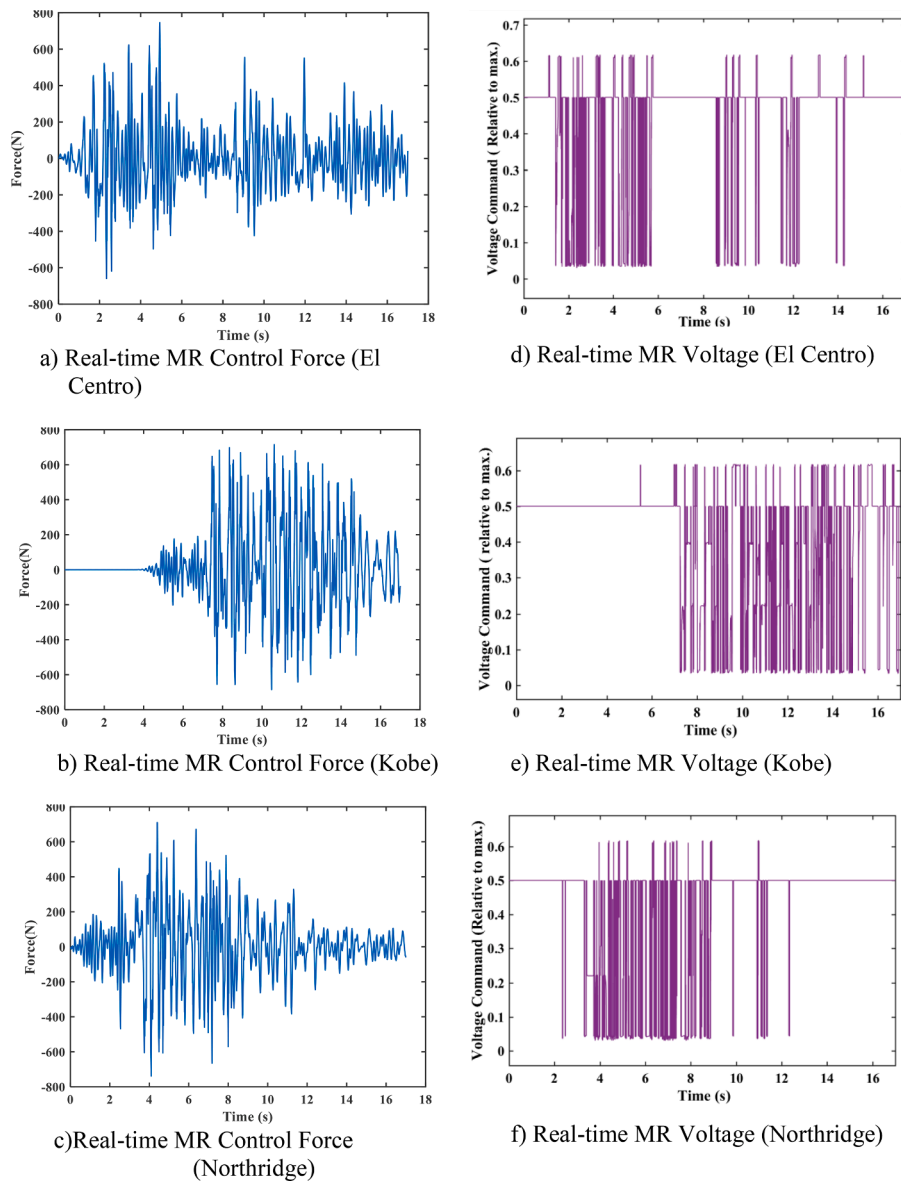


Fig. 17. Real-time MR control force and commanding voltage under different earthquakes.

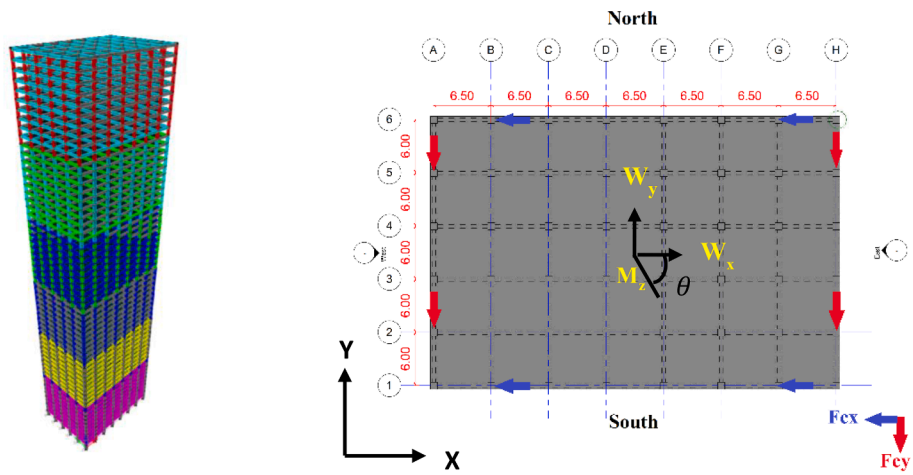


Fig. 18. Plan and 3D views for the 60 story wind excited building.

**Table 9**  
Structural members properties of the 60 story high rise building.

Member	Cross Section(mm)	Story
Corner column	750×750	51st – 60th
	750×750	41st – 50th
	800×800	31st – 40th
	850×850	21st – 30th
	900×900	11th – 20th
	1100×1100	1st – 10th
Non-corner column	750×750	51st – 60th
	750×750	41st – 50th
	800×800	31st – 40th
	850×850	21st – 30th
	900×900	11th – 20th
	1100×1100	1st – 10th
Exterior Beams	400×700	51st – 60th
	400×700	41st – 50th
	450×750	31st – 40th
	500×750	21st – 30th
	550×750	11th – 20th
	550×800	1st – 10th
Interior Beam	400×700	51st – 60th
	400×700	41st – 50th
	450×750	31st – 40th
	500×750	21st – 30th
	550×750	11th – 20th
	550×800	1st – 10th

**Table 10**  
Structural Modal Properties (Wind Excited Structure).

Mode	Period (s)	Frequency (cycle/s)
1	5.228	0.191
2	4.125	0.242
3	2.414	0.414
4	1.359	0.736
5	1.212	0.825
6	0.917	1.090

multi-objective functions is employed by defining below objectives functions:

$$\begin{aligned} \text{Minimize: } f_1 &= \frac{1}{nm} \sum_{j=1}^m \sum_{i=1}^n \max(|\text{drift}_{ij}(t)|) \\ f_2 &= \frac{1}{nm} \sum_{j=1}^m \sum_{i=1}^n \max(|\text{acc}_{ij}(t)|) \end{aligned}$$

$$i = 1, 2, 3, \dots, nt = 1, 2, 3, \dots, t_{max} \tag{13}$$

Where  $f_1, f_2$  is the proposed objective functions,  $i$  is the  $i^{\text{th}}$  story,  $\text{drift}_i(t)$  and  $\text{acc}_i(t)$  are the corresponding inter story drift and absolute acceleration at time ( $t$ ) respectively,  $j$  is the corresponding earthquake or load component.

**2.4.1. Constraints and penalty function**

One inequality constraint was defined for each objective function, it is simply defined as:

$$f_1 < \frac{1}{nm} \sum_{j=1}^m \sum_{i=0}^n \max(|\text{drift}_{i^*}(t)|)$$

$$f_2 < \frac{1}{nm} \sum_{j=1}^m \sum_{i=0}^n \max(|\text{acc}_{i^*}(t)|) \tag{14}$$

$\text{drift}_{i^*}(t)$  and  $\text{acc}_{i^*}(t)$  is the uncontrolled story drift and story acceleration, respectively,  $j$  is corresponding earthquake or load component.

To penalize undesired universe that does not meet the constraints,

following equation were employed:

$$f(r) = f(r) + \lambda^2 \psi \tag{15}$$

Where  $f(r)$  is the  $r^{\text{th}}$  objective function,  $\lambda$  is penalty constant ( $=10^{15}$ ),  $\psi$  is inequality function returning zero when the constraint is confirmed and one when the constraint is violated.

**2.5. Other control strategies**

For the purposes of comparison, two well-known semi-active vibration control strategies, Clipped Optimal (CO) and Modified quasi Bang-Bang (MBB), were used. These two algorithms are briefly described as follows:

**2.5.1. Clipped optimal**

One of the most well-known semi-active vibration control algorithms is the Clipped Optimal (CO) algorithm, which was presented by Dyke et al. [19]. This algorithm is based on the optimal control force produced by a linear optimal controller (such as LQR or LQG). The CO algorithm commands the current driver of the MR damper with the desired command voltage in real-time, depending on the response and control force feedback signals:

$$f_c = L^{-1} \left\{ -K_c(s)L \left\{ \begin{matrix} y \\ f \end{matrix} \right\} \right\}, \tag{16}$$

Where  $f_c$  is the optimal control force,  $L\{\cdot\}$  is the Laplace transform,  $K_c$  is the optimal feedback gain,  $y = [\ddot{x}_1, \ddot{x}_2, \ddot{x}_3, x_1]$  are the vector of feedback floors' acceleration response and the first floor displacement, respectively.  $f$  is the feedback control force generated by MR damper.

The control law can be expresses as:

$$V_i = \begin{cases} V_{i-1}, f = f_c \\ V_{max}, f \leq f_c | \text{sign}(f) = \text{sign}(f_c) \\ 0, \text{otherscases} \end{cases} \tag{17}$$

$V_i$  is the instant commanding voltage.

In this paper, a Linear Quadratic Regulator (LQR) controller was utilized to obtain the optimal response gain. Following Dyke et al. [19], only the top floor response was taken into consideration, therefore the Q matrix was set to zero except for Q33, which was set to 1. The optimal Q and R multipliers of  $10^{17}$  and 1, respectively, were determined through a trial-and-error approach using the (lqr) function in MATLAB for the structure excited by the El Centro earthquake.

**2.5.2. Modified quasi Bang-Bang**

The Quasi Bang-Bang control algorithm relies on passive-off and passive-on control states as control commands based on the direction of building movement, either towards or away from its static equilibrium. To improve upon this approach, Aly [4] proposed a modified Quasi Bang-Bang control strategy for semi-active vibration control structural systems equipped with MR dampers. In contrast to the clipped optimal and Quasi Bang-Bang strategies, the Modified Bang-Bang (MBB) approach uses a range of commanding voltage between 0 and the maximum value based on the structural feedback response. This approach can be expressed as follows:

$$V_i = \begin{cases} \alpha_c V_{max}, (\text{sign}(x) = 1, \text{sign}(\dot{x}) = 1) \\ \beta_c V_{max}, (\text{sign}(x) = -1, \text{sign}(\dot{x}) = -1) \\ \gamma_c V_{max}, (\text{sign}(x) = 1, \text{sign}(\dot{x}) = -1) \\ V_{max}, \text{otherscases} \end{cases} \tag{18}$$

$\alpha_c, \beta_c$ , and  $\gamma_c$  are coefficients between 0 and 1. However, for the sake of comparison the value of 0, 0.11 and 0.4 are employed, respectively, Aly [4].

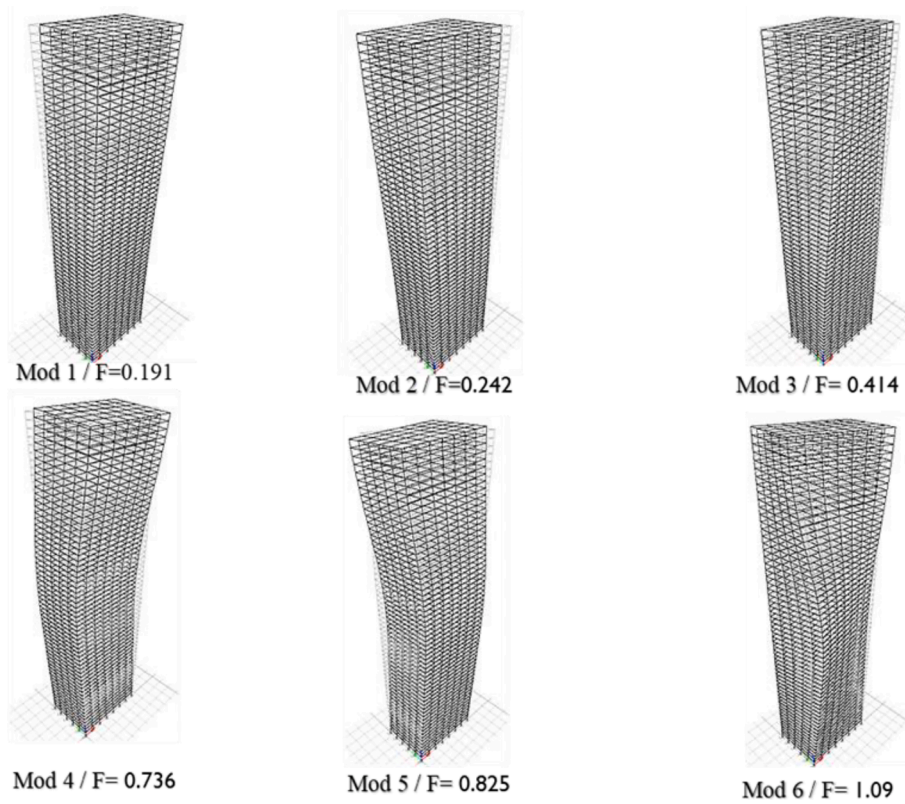


Fig. 19. The Considered Modes Shapes for The 3D Numerical Application.

**Table 11**  
Optimization Parameters for Wind Excited Structural Vibration Control System.

Parameter	Value
3	Number of Iterations
20	Number of Universes
100	Archive Size
3	Number of independent iterations
2	Objective functions
110	Number of design variables

### 3. Numerical applications

The developed method has been applied to a three-story structure under earthquake excitation and a sixty-story structure subjected to multi directional wind loads. In the following subsections a detail of applications is presented.

#### 3.1. Three story shear building

To evaluate the performance of the developed vibration control system and compare it with other control methods, a three story structure is considered which has been used in previous studies at the

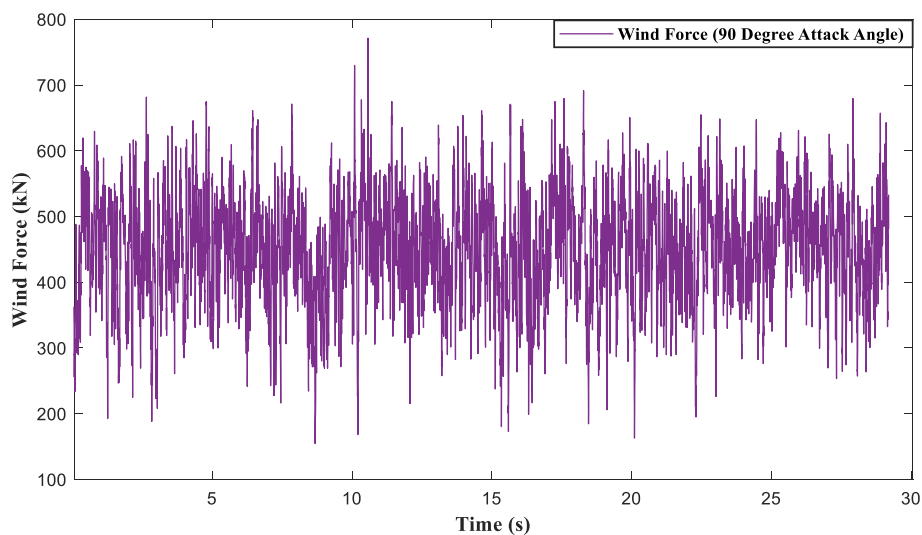


Fig. 20. Along Wind Time History Load At Top Story.

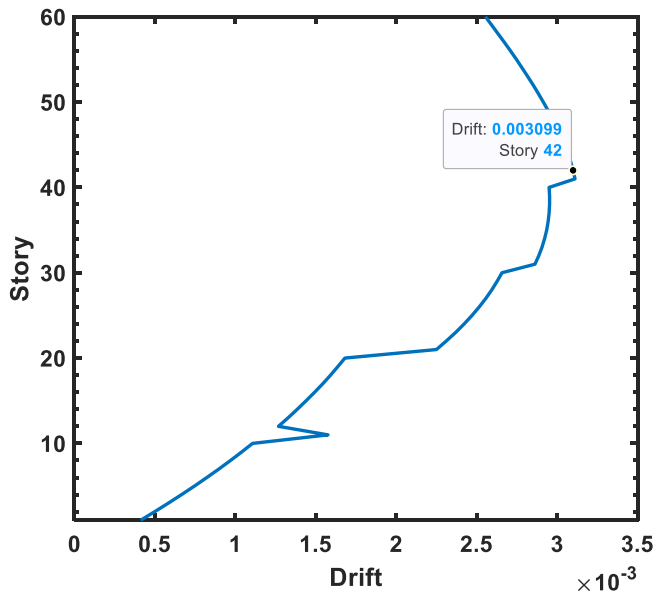


Fig. 21. First Mode Maximum Story Drift Along Y-Axis.

Structural Dynamics and Control/Earthquake Engineering Laboratory (SDC/EEL) at the University of Notre Dame Aly [4]. It is a scaled model of a prototype structure with a steel frame of 158 cm in height and 227 kg of total mass distributed evenly along the floors Dyke et al. [20]. Fig. 8 shows a schematic for the scaled model of the benchmark structure.

The building structure was modelled as a state space system (see Section 3.3.1), and the analytical model of the MR damper was integrated on the first floor (see Section 2.2). The FLMVOC algorithm was then implemented in MATLAB and SIMULINK to control the system.

3.1.1. Governing equation of motion

The governing equation for earthquake excited structure with control devices is given by:

$$M_{nn}\{\ddot{x}\}_{n1} + C_{nn}\{\dot{x}\}_{n1} + K_{nn}\{x\}_{n1} = -M_{nn}\{\Lambda\}\ddot{x}_g + \{\Gamma\}f \tag{19}$$

Where  $M$  represents a structure mass matrix,  $C$  is the structure damping matrix,  $K$  is the stiffness matrix,  $\{x\}$ ,  $\{\dot{x}\}$ ,  $\{\ddot{x}\}$  are the vectors of floors' displacement, velocity and acceleration, respectively,  $\{\Lambda\}$  is a vector of ones implements  $\ddot{x}_g$  which is a one dimensional horizontal ground acceleration,  $\{\Gamma\}$  is a vector of dampers locations defined by 0 or 1,  $f$  is the control force generated in MR damper.

The state space representation of the dynamic system is defined as:

$$\begin{aligned} \dot{z} &= Az + Bf + E\ddot{x}_g \\ y &= Cz + Df \end{aligned} \tag{20}$$

Where  $z$  is the state vector;  $A$ ,  $B$ ,  $C$ ,  $D$ , and  $E$  are state space matrices;  $f = [f_1, f_2, f_3, \dots, f_n]^T$  is a vector of measured control forces;  $y$  is the

measured output and  $n$  is the number of degrees of freedom (number of storeys for one dimensional structural model).

The damper is assumed to be attached rigidly between the first floor and the ground so that the velocity response of the damper is equal to the response of the first floor. Since a full structural response observation was assumed, then  $y = \{\ddot{x}_1, \ddot{x}_2, \ddot{x}_3, x_1, x_2, x_3, \dot{x}_1, \dot{x}_2, \dot{x}_3\}^T$  and the matrices for the state space representation of the system are formulated and shown by the Eq. (18):

$$\begin{aligned} A &= \begin{bmatrix} 0_{n \times n} & I_{n \times n} \\ -M^{-1}K & -M^{-1}C \end{bmatrix}, C = \begin{bmatrix} M^{-1}K & M^{-1}C \\ I_{n \times n} & 0_{n \times n} \\ 0_{n \times n} & I_{n \times n} \end{bmatrix}, \\ B &= \begin{bmatrix} 0_{1 \times n} \\ M^{-1}\Gamma \end{bmatrix}, D = \begin{bmatrix} M^{-1}\Gamma \\ 0_{2n \times n} \end{bmatrix}, E = - \begin{bmatrix} 0_{1 \times n} \\ I_{1 \times n} \end{bmatrix} \end{aligned} \tag{21}$$

The structure properties presented in literatures Aly [4,18,19] were employed here, Eq. (22):

$$\begin{aligned} M &= \begin{bmatrix} 98.3 & 0 & 0 \\ 0 & 98.3 & 0 \\ 0 & 0 & 98.3 \end{bmatrix} kg \\ C &= \begin{bmatrix} 175 & -50 & 0 \\ -50 & 100 & -50 \\ 0 & -50 & 50 \end{bmatrix} N \cdot \frac{s}{m} \\ K &= \begin{bmatrix} 12 & -6.84 & 0 \\ -6.84 & 13.7 & -6.84 \\ 0 & -6.84 & 6.84 \end{bmatrix} \times 10^5 \frac{N}{m} \end{aligned}$$

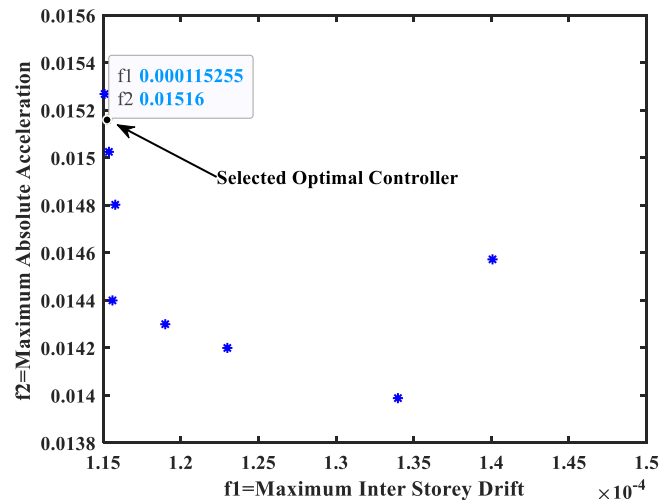


Fig. 22. Pareto Optimal FLC Controllers for Wind-Excited Structure.

Table 12 Base Rules' Weights for the Optimal FL Controller.

Drift	Acceleration						
	LN	N	SN	Z	SP	P	LP
LN	MV0.9779	MV0.4368	NV0.0953	NV0.2091	NV0.4312	MV0.3361	MV0.8540
N	NV0.7619	NV0.2062	MeV0.2375	MeV0.6143	MeV0.0849	NV0.7285	NV0.0679
SN	MeV0.1123	MeV0.5440	LV0.3119	LV0.1821	LV1	MeV0	MeV0.8085
Z	MeV0	LV0.3272	LV0.8998	LV0	LV0.3272	LV0.8008	MeV0.1345
SP	MeV0.5924	MeV0.6038	LV0.2261	LV0.5417	LV0.7350	MeV0.7771	MeV0.6261
P	NV0.5085	NV0	MeV0.7191	MeV0.1556	MeV0.6628	NV0.6543	NV0.5387
LP	MV0.1303	MV0.9530	NV0.5720	NV0.9571	NV0.6440	MV0.8302	MV0.5739

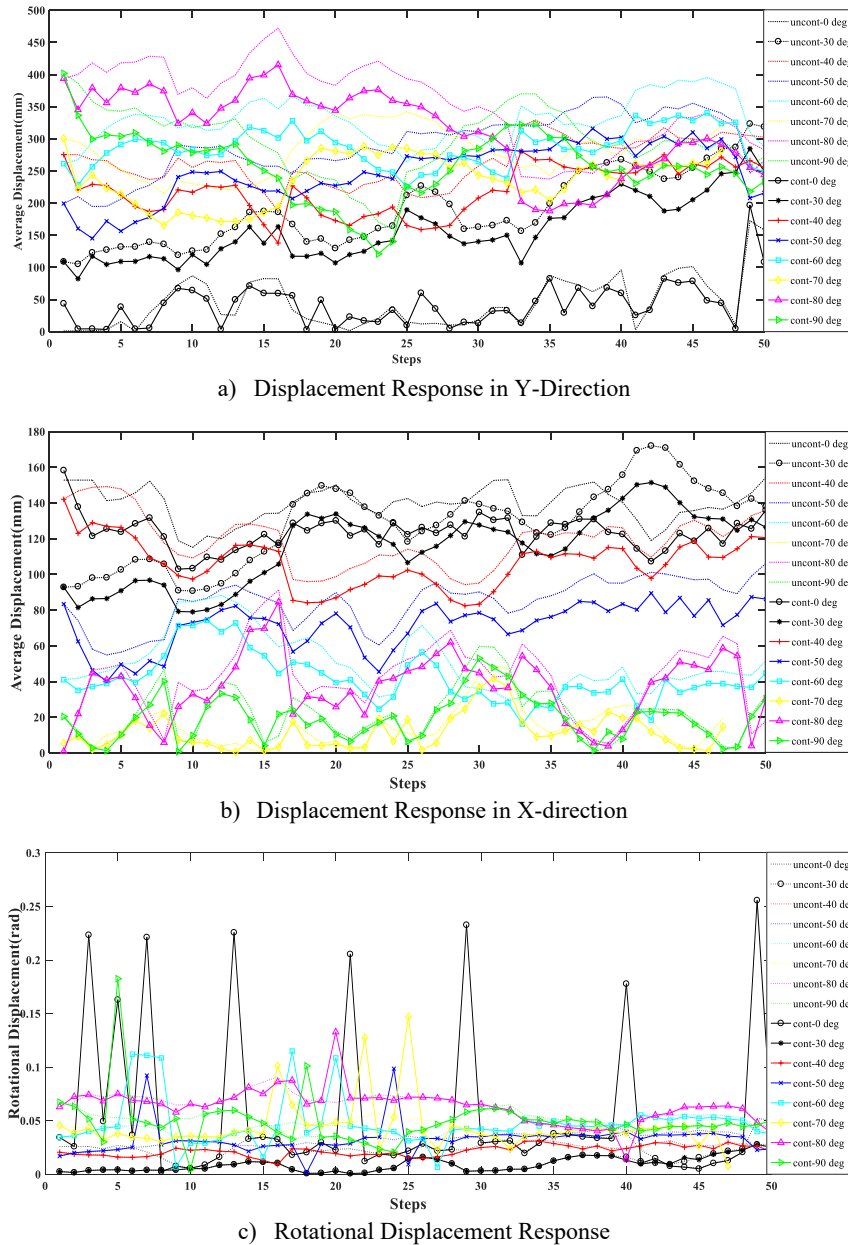


Fig. 23. Uncontrolled and Controlled Displacement Response under Multidirectional Wind Load.

$$\Gamma = \begin{bmatrix} 1 \\ 0 \\ 0 \end{bmatrix}, \Lambda = \begin{bmatrix} 1 \\ 1 \\ 1 \end{bmatrix} \quad (22)$$

The damping matrix has been calculated using Rayleigh Method for the first two modes with a five percent damping ratio. However, the values shown in Eq. (19) are used for verifying purpose.

### 3.1.2. Earthquakes time history records

The considered structure is assumed to be subjected to three earthquake time history excitations include of one far-field and two near-field earthquakes. Therefore, the following earthquake records applied to the three-story structure:

- i) El Centro earthquake, 1940 (PGA = 0.348 g): The N-S component recorded at the Imperial Valley Irrigation District substation in El Centro, California, during the Imperial Valley, California earthquake of May 18, 1940.

- ii) Kobe earthquake, 1995 (PGA = 0.834 g): The N-S component recorded at the Kobe Japanese Meteorological Agency (JMA) station during the Hyogoken Nanbu earthquake of January 17, 1995.

- iii) Northridge earthquake, 1994 (PGA = 0.843 g): The N-S component recorded at Sylmar County Hospital parking lot in Sylmar, California, during the Northridge, California earthquake of January 17, 1994.

Fig. 9 shows the accelerations for the considered earthquakes.

### 3.1.3. Optimal controller by FLMVOC

In order to get the optimal Fuzzy Logic controller and deploy it in the structural system, the formulated Fuzzy Logic controller has trained with the proposed optimization method presented in section 2.1.2 under the effect of seismic loads (section 3.1.2). Then the optimal controller is selected among the Pareto optimal solutions. The Pareto optimum

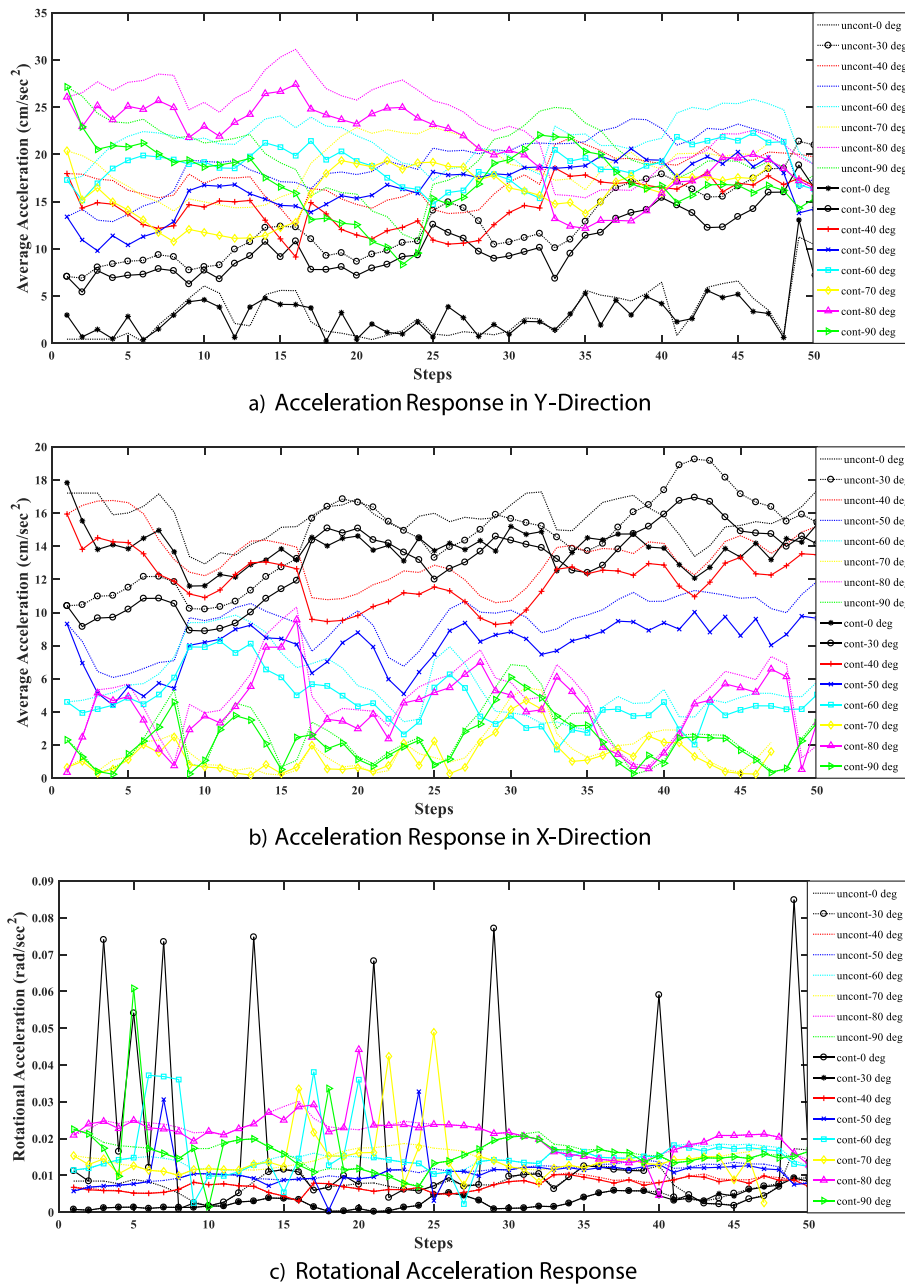


Fig. 24. Uncontrolled and Controlled Acceleration Response under Multidirectional Wind Load.

solutions and the optimization criteria are shown in Fig. 10 and Table 7, respectively.

It is clear from the optimization results that there is no significant difference between the solutions over all iterations since there is a slight change in the values of the objective functions. This gives a good sense of the powerful performance of the proposed algorithm as it can produce a good solution after a few iterations. Base rules' weights and membership functions for the optimized controller are shown in Table 6.

### 3.1.4. Results and discussion

The real-time response has been obtained to assess the performance of the developed semi-active vibration control system. The maximum response has been compared with the well-known Clipped-Optimal(CO) and Modified Bang-Bang (MBB) semi-active vibration control strategies Aly [4], as well as the Passive-On control case, the comparison results are shown in Table 8. The results indicated that a competitive performance of the developed FLMVOC system in mitigating the story drift and

absolute acceleration along all structure stories. FLMVOC demonstrated an average reduction of 44% in top story drift and absolute acceleration when subjected to diverse earthquake amplitudes. Under the effect of the El Centro earthquake, the maximum reductions in top story drift and absolute acceleration were similar for both CO and MBB strategies, equal to 44% and 48%, respectively. However, FLMVOC showed superiority over other control strategies when the structure was excited by the near-field high-magnitude Northridge earthquake, as shown in Figs. 11 and 12. FLMVOC is superior in terms of robustness and adaptivity compared to reference control strategies as it utilizes a single controller that can withstand uncertainties in excitation and provide rational response control action. Unlike reference control strategies, FLMVOC doesn't require parameter changes to adapt to uncertainties, making it more adaptive and efficient. Furthermore, FLMVOC strategy demonstrated significant power-saving capabilities and effectively utilized control force compared to the CO and MBB strategies. It achieved efficient control action by using only 52–67% of the control force

**Table 13**  
Maximum Building's Response under the Effect of Multi Directional Wind Load.

Response Type*		Wind Load Attack Angle							
		0°	30°	40°	50°	60°	70°	80°	90°
Drift-X	Controlled	1.900E-03	<b>1.768E-03</b>	<b>1.685E-03</b>	<b>1.060E-03</b>	<b>8.507E-04</b>	<b>5.074E-04</b>	<b>1.022E-03</b>	<b>6.946E-04</b>
	Uncontrolled	1.860E-03	2.017E-03	1.785E-03	1.249E-03	1.023E-03	5.878E-04	1.102E-03	7.737E-04
Drift-Y	Controlled	<b>2.473E-03</b>	<b>3.586E-03</b>	<b>3.530E-03</b>	<b>3.935E-03</b>	<b>4.249E-03</b>	<b>3.699E-03</b>	<b>5.219E-03</b>	<b>4.326E-03</b>
	Uncontrolled	2.154E-03	4.067E-03	4.134E-03	4.536E-03	1.632E-03	4.337E-03	5.928E-03	5.135E-03
Displacement-X	Controlled	<b>1.379E-01</b>	<b>1.515E-01</b>	<b>1.421E-01</b>	<b>8.950E-02</b>	<b>7.433E-02</b>	<b>4.177E-02</b>	<b>8.451E-02</b>	<b>5.300E-02</b>
	Uncontrolled	1.530E-01	1.720E-01	1.492E-01	1.012E-01	8.825E-02	4.862E-02	9.126E-02	5.975E-02
Displacement-Y	Controlled	1.967E-01	<b>2.847E-01</b>	<b>2.810E-01</b>	<b>3.160E-01</b>	<b>3.405E-01</b>	<b>2.883E-01</b>	<b>4.151E-01</b>	<b>3.365E-01</b>
	Uncontrolled	1.726E-01	3.234E-01	3.293E-01	3.652E-01	3.955E-01	3.420E-01	4.722E-01	4.020E-01
Rotational Displacement	Controlled	2.557E-04	2.790E-05	3.094E-05	9.855E-05	1.150E-04	1.470E-04	1.327E-04	1.826E-04
	Uncontrolled	5.204E-05	2.778E-05	3.219E-05	4.306E-05	5.624E-05	5.598E-05	9.079E-05	6.731E-05
Acceleration-X	Controlled	<b>1.585E-01</b>	<b>1.701E-01</b>	<b>1.460E-01</b>	<b>1.021E-01</b>	<b>8.417E-02</b>	<b>4.866E-02</b>	<b>9.911E-02</b>	<b>6.339E-02</b>
	Uncontrolled	1.758E-01	1.931E-01	1.685E-01	1.200E-01	1.009E-01	5.627E-02	1.070E-01	7.101E-02
Acceleration-Y	Controlled	1.397E-01	<b>1.893E-01</b>	<b>1.863E-01</b>	<b>2.069E-01</b>	<b>2.238E-01</b>	<b>2.048E-01</b>	<b>2.759E-01</b>	<b>2.729E-01</b>
	Uncontrolled	1.138E-01	2.143E-01	2.180E-01	2.385E-01	2.596E-01	2.298E-01	3.132E-01	3.054-01
Rotational Acceleration	Controlled	8.490E-04	9.326E-05	1.024E-04	3.279E-04	3.810E-04	4.889E-04	4.421E-04	6.085E-04
	Uncontrolled	1.728E-04	9.331E-05	1.068E-04	1.420E-04	1.858E-04	1.868E-04	3.020E-04	2.259E-04
Rotational Velocity**	Controlled	3.039E-01	3.313E-02	3.676E-02	1.171E-01	1.367E-01	1.747E-01	1.578E-01	2.170E + 00
	Uncontrolled	6.188E-02	3.321E-02	3.825E-02	5.112E-02	6.796E-02	6.657E-02	1.079E-01	8.007E-02

Notes:

\* Drift's values are unit less, acceleration values are in (m/s<sup>2</sup>), rotational acceleration is in (rad/s<sup>2</sup>), rotational velocity is in (milli-rad/s).

\*\* Permissible Acceleration = 20 milli-g (0.2 m/s<sup>2</sup>), Permissible Rotational Velocity = 5 milli-rad/s [7].

produced by the reference control strategies. Fig. 13(a – c) present the real-time third-floor response and the produced MR control force under the effect of the El Centro earthquake, demonstrating the competitive performance of FLMVOC compared to other control strategies.

Table 6 shows the base rules weights for the selected optimal fuzzy logic controller. As it can be seen, the high weight value (70–98) % has primarily been assigned to the maximum voltage membership function (MV). Meanwhile, the low voltage membership function (LV) has been assigned with a low weight percentage in the range of (0–30) %; this indicates the reliability of the formulated fuzzy logic controller and the optimization methodology.

Fig. 14 shows the maximum structural response to the considered earthquakes. The maximum relative story displacement for the uncontrolled structure is about 6 mm under the effect of El Centro earthquake and 10 mm under both the Kobe and Northridge earthquakes. Despite the high disparities in the intensity between far-field and near-field earthquakes (about 200%), the developed control system has effectively mitigated the structural response for all considered load cases.

The first story real-time response (Figs. 15 and 16) proves the outstanding performance of the control system to diminish the structural response in real-time include of both floors' drift and acceleration when the seismic excitation is applied to the structure.

It can be seen from Table 8 that the reduction in story drift at the first floor for the structure utilized with the developed FLMVOC control system excited by El Centro, Kobe, and Northridge earthquakes are 60%, 53%, and 41%, respectively. In contrast, the average drift reduction for the three floors is 50%, 51%, and 37% under the effect of El Centro, Kobe, and Northridge earthquakes, respectively.

As indicated in Table 8, the reduction in story drift for the second and third floors is 45% and 44%, respectively. At the same time, the reduction in absolute acceleration is 31% and 45% for the mentioned

floors, under the effect of El Centro earthquake. The same structural behaviour has been observed for other applied earthquakes.

Considering the absolute acceleration response, FLMVOC control system has successfully reduced the structural acceleration at the controlled (first) floor by 38%, 17%, and 10% under the effect of El Centro, Kobe, and Northridge earthquakes, respectively. However, it can be indicated that the reduction in acceleration is inversely proportional to the earthquake intensity.

Albeit the contradictory relationship between the story drift and story acceleration as reducing one can violate the other Joghataie et al. [27], the developed FLMVOC is successfully overcome this response interaction by adequate formulation of fuzzy logic base rules which minimizing the story acceleration as much possible without violating the story drift. Despite of deploying MR damper in the only first floor, the control system effectively mitigated the response of all other floors by dissipating the applied ground motion energy in the first floor.

The results in Fig. 17 present the real-time control force and commanding voltage produced by the MR damper. It can be seen the power of the developed FLMVOC to respond in real-time under the effect of the considered earthquakes. Compared with the reference control strategy, FLMVOC has allocated only 87.7% of the reference control force to command the MR damper, reflecting the competitive performance of FLMVOC in commanding and exploiting the control force. Furthermore, the saturation state of MR damper (i.e. the control capacity at which increasing of driven voltage is no longer affect MR Fluid characteristics) is implicitly avoided by the FL controller allocating approximately 2 V of the MR driver keeping it below 2.25 V [20]. This reflects the outstanding power-saving feature of FLMVOC. However, this behaviour is expected to be even more accurate by utilizing higher order of FL membership functions. The maximum produced control force for near-field earthquakes is less than for far-field earthquakes, which proves the capability

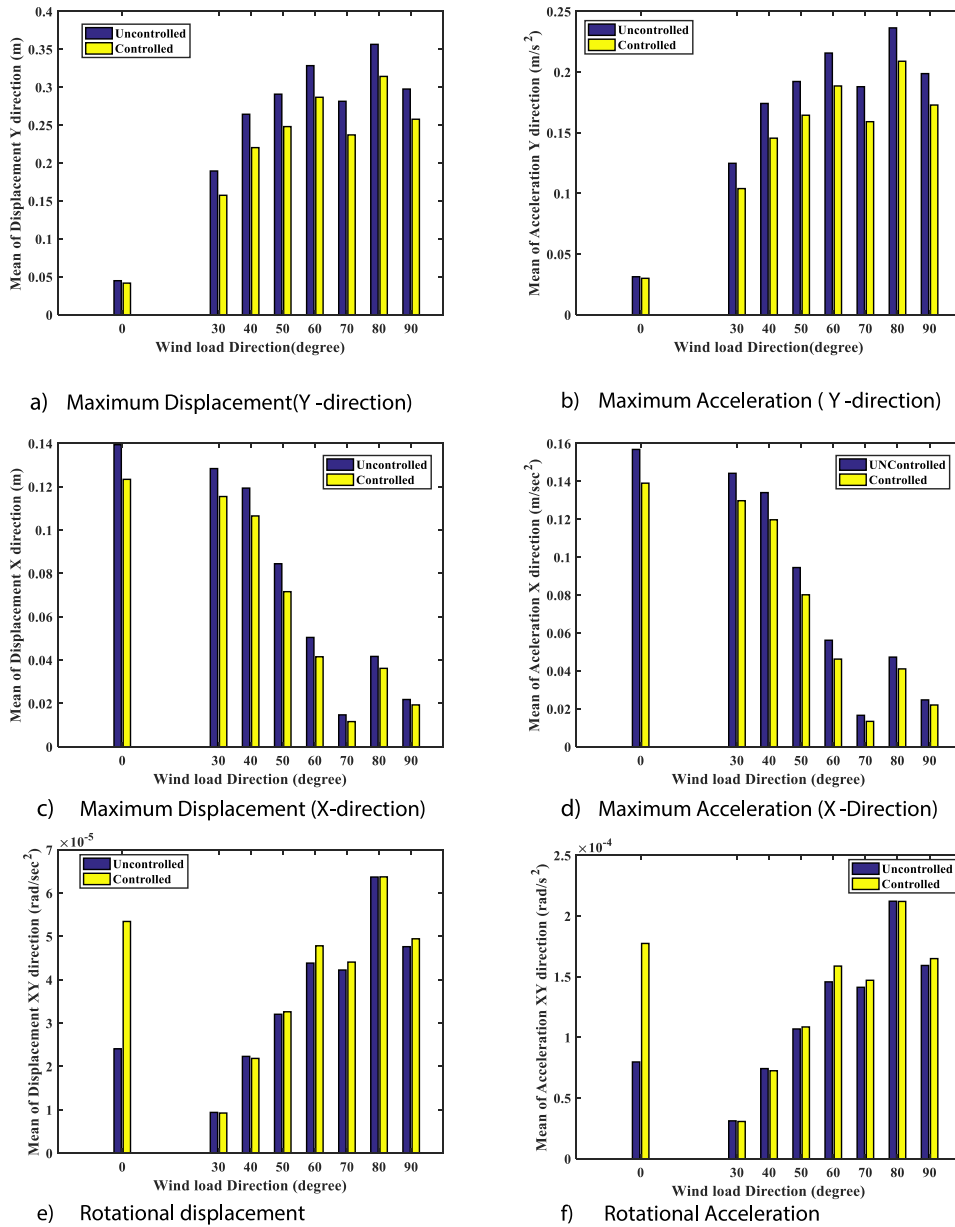


Fig. 25. A comparison between controlled and uncontrolled maximum response values.

of FLMVOC to adapt and manage the commanding MR voltage very well by maintaining a sound reduction in story acceleration, keeping the reduction in story drift as high as possible.

### 3.2. Sixty story high rise building

To evaluate the robustness of the proposed control mechanism against uncertainties in external load and multi-dimensional structural response. The developed FLMVOC control system has been utilized to control the response of a 60-story reinforced concrete building. The following sections are demonstrating the structural and simulation properties in detail.

#### 3.2.1. Structure properties

The selected building is well known as the CAARC building (Melbourne 1980) [36]. The structure is 45.72 m in width, 30.48 m in depth, and 182.88 m in height. The structure consists of seven by five bays. It is

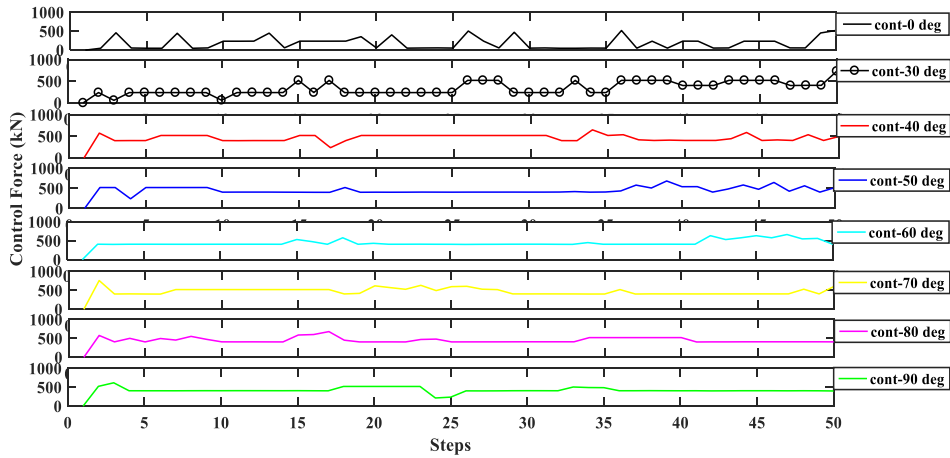
a moment-resisting system and contains 2880 columns and 4920 beams. its floors are assumed to be rigid diaphragms.

The building is considered to be stationed at a hurricane prone area near Melbourne, Florida. The orientation angle of the building is 270° clockwise from the north, i.e., the front façade faces the north. Fig. 18 shows the plan and 3D views of the considered structure.

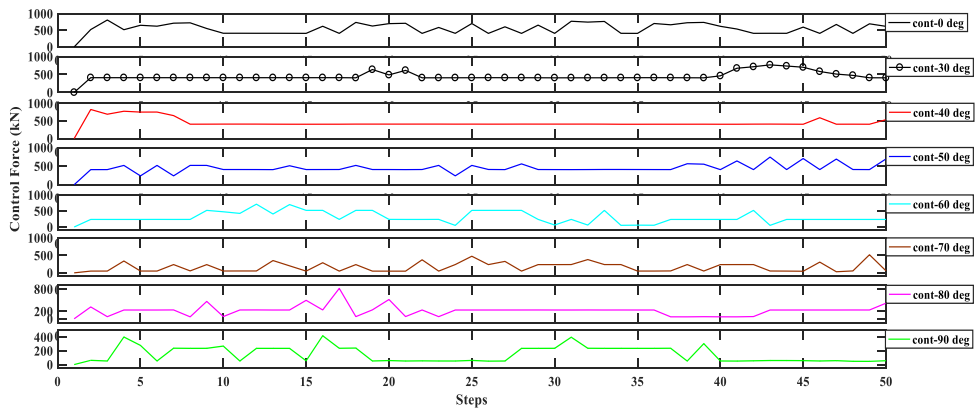
The structural members' properties are shown in Table 9, the concrete density of 25 kN/m³ is used, and a compression strength of 60 MPa is assumed.

The analysis is conducted using ETABS software by utilizing ETABS oAPI (Open Application Programming Interface) [11,15] during the optimization process and later on during full simulation for the controlled structural system with optimal controller. Linear Modal Time history analysis is employed to simulate the structure at each time step.

The structural analysis has been performed by employing only the first six modes of vibration to decrease the simulation time. However, the considered modes have been found to participate in more than 80%



a) Real-time Control Force Along Y direction



b) Real-time Control Force Along X-direction

Fig. 26. Real-time Commanded Control Force by FLMVOC Control System.

of the structural response of the orthogonal directions. A damping ratio of 2% has been adopted for all six modes. Table 10 and Fig. 19 show the modal properties for the considered structure. Table 11.

A ramp time history function has been defined to trace the dynamic action of the applied load at each time step. A pulse width equal to the load time sample is utilized. Then, the ramp function is assigned to the modal time-history load case for all dynamic load components. An initial analysis was conducted, then after, the structural response was compared with the result from static analysis, which it found satisfactory with the requirements of the ASCE code [6].

### 3.2.2. Wind load time history

The wind tunnel pressure coefficients from High Rise Database Assisted Design (HR-DAD)[43,36] were employed. The building is assumed to be located in a type C exposure area. The pressure coefficients were measured in wind tunnel tests at the Prato (Italy) Inter-University Research Centre on Building Aerodynamics and Wind Engineering (CRIAC IV-DIC) Boundary Layer Wind Tunnel.

The hourly mean speed at the top floor for the building model in the wind tunnel test was 23.2 m/s, a hurricane wind speed of 67.5 m/s for 1700 years MRI (Table C26.5-3), [6] has been assumed, and the wind load time history has been scaled using following formulas:

$$\bar{V} = \bar{b} \left( \frac{\bar{Z}}{10} \right)^{\bar{\alpha}} V \tag{23}$$

Where  $V$  is the basic wind speed corresponds to a 50-years mean recurrence interval at 10 m aboveground and for exposure category C (or 3sec gust speed),  $\bar{V}$  is mean hourly design wind speed,  $\bar{Z}$  is effective structure height ( $=0.6 \times \text{considered height}$ ),  $\bar{b}$  is Gust factor 1/F at 10 m,  $\bar{\alpha}$  is a power law exponent of mean wind speed profile.

In this research, a values of 110 m ( $0.6 \times 182.88$ ), 0.65, and 0.153 for  $\bar{Z}$ ,  $\bar{b}$  and  $\bar{\alpha}$  respectively, were adopted. The scale factor is obtained using following formula [17]:

$$K_v = \left( \frac{U}{U_r} \right)^2 \tag{24}$$

Where  $K_v$  is the design wind speed scale factor,  $U$  is the design mean wind speed at top floor and  $U_r$  is the reference hourly mean wind speed (i.e., 23.2 m/sec).

Bernoulli’s equation for fluid was utilized to calculate the load from pressure coefficients after scaling, it is defined as follows:

$$P = C_p 0.5 \rho \bar{V}^2 A_f \tag{25}$$

Where  $P$  is the wind load,  $C_p$  is the pressure coefficients,  $\rho$  is air mass density ( $1.25 \text{ kg/m}^3$ ) and  $A_f$  is the floor area.

Three components of wind load records, X-direction, Y-direction and rotational load, have been used during both optimization and evaluation stages. These records include multi directional wind for all floors (i.e.  $\theta_i = 0^\circ, 30^\circ, 40^\circ, 50^\circ, 60^\circ, 70^\circ, 80^\circ, \text{ and } 90^\circ$ ), where  $i$  is the  $i^{\text{th}}$  floor.

However, to avoid confusion, only the wind load for the top story and for  $\theta = 90^\circ$ , i.e. along wind case, was plotted and shown in Fig. 20.

Since the wind pressure coefficients are calculated and corrected to be exerted on the centre of the floor [43], wind load components are also applied as a point load in the centre of floor(diaphragm), Fig. 18.

It is worth mentioning that the optimum number of dampers is not intended in this study. Hence, four dampers in each direction are assumed at selected points, Fig. 18.

Since the proposed controller has been fed with a story drift as one of the controller inputs, story 42 has been selected to be the study floor as it is seen from the initial analysis that it has the maximum story drift for the considered vibration modes, Fig. 21.

### 3.2.3. Optimal controller for wind-excited structure

Following the previously stated procedures of the proposed optimal fuzzy logic controller strategy (FLMVOC), the optimization has been run by utilizing ETABS oAPI to integrate the different simulation environments of the controller and 3D structure; this is done by accessing a.NET dynamic link library form of API from MATLAB as.NET client.

The developed fuzzy logic controller in section 2.1 has been implemented; however, in contrast to earthquake excited structures, controlling the acceleration is more critical design criterion in the wind excited structure. Therefore, the fuzzy rules have been formulated to focus more on controlling acceleration by commanding a large control force when high values of structural acceleration response happen, regardless of the story drift values.

Fig. 2 and Table 2 show the proposed membership functions and the base rules, respectively.

Because of the high computational power consumption of a 3D simulation, only 5-time steps have been used during optimization process, however, a set of fifty time steps is employed to simulate the structure furnished with the optimal controllers, Table 12 shows the optimization parameters for the wind excited problem.

The optimal controller is chosen amongst the Pareto optimal solutions which have been obtained by the optimization processing, then it has been implemented at each control point in the concerned floor (section 3.2.1). After that, the simulation has been done for the system excited by a complete set of wind load records (section 3.2.2). Fig. 22 and Table 12 show the Pareto optimal solutions and the produced base rules' weights for the optimal controller, respectively.

### 3.2.4. Results and discussion

The developed optimal fuzzy logic controller is deployed in the high-rise building as stated in section 3.2.1. For the sake of efficient control performance in each response component (i.e., along wind, across wind and rotational), and owing to the discrepancy between across wind and along wind structural response, the concept of decentralized system was applied by implementing one controller for each MR damper at the selected eight control points (four in X-Direction and four in Y-Direction).

Real-time response due to the three load components with multiple load directions ( $\theta = 0^\circ, 30^\circ, 40^\circ, 50^\circ, 60^\circ, 70^\circ, 80^\circ, 90^\circ$ ) is compared with the corresponding uncontrolled response. Fig. 23(a – c) and Fig. 24(a – c) show the average response of four points in each direction, while the rotational response is related to the average of all control points.

Since the structure's occupant category is office building [36], a threshold of 20 milli-g for the floor's acceleration response is utilized [7] in mapping the acceleration membership functions of the FLC. In the same way, the values of maximum uncontrolled story drift and maximum voltage capacity for the MR damper's current driver are used in mapping the membership functions for the drift and commanding voltage, respectively.

Feature of defining input and output membership function relative to design values, enables us to implement the controller in any structural system. Furthermore, it offers a tuning tool without the need to run

optimization processing since the system performs sufficiently.

It can be seen in Fig. 23 and Fig. 24 that the controller is effectively controlled the response at each time step keeping it within the permissible limits (10 mm for story drift and  $0.2\text{--}0.25\text{ m/s}^2$  for acceleration) in both along wind and across wind directions. Although the rotational response is found over the uncontrolled response when pure along wind load case happens, it was minimal in value and had not exceeded the thresholds of (5 milli-rad/s) specified in ATC Design Guide 3 [7].

Table 13 shows the building's maximum response considering different load directions. The percentage of reduction in floor's displacement along Y-axis are 12.0%, 14.7%, 13.5%, 13.9%, 15.7%, 12.1%, and 16.3% under the effect of wind attack angles of  $0^\circ, 30^\circ, 40^\circ, 50^\circ, 60^\circ, 70^\circ, 80^\circ$  and  $90^\circ$  respectively. Similarly, reduction in acceleration response along Y-axis had been of 11.8%, 14.6%, 13.3%, 13.8%, 15.4%, 11.9%, and 15.6% respectively.

For the ( $0^\circ$ ) wind attack angle, a leap in both displacement and acceleration response in Y-direction can be observed at several time steps; however, its values are relatively small and do not exceed the allowable limits. Fig. 25(a – f) shows a comparison between controlled and uncontrolled maximum displacement response.

The destabilization state of the structural control system deployed with semi-active dampers would not happen in a real application; hence, there is more than one reason that can interpret the system behavior under the effect of the ( $0^\circ$ ) component of wind load. Firstly, the difference in building dimension results in a strong effect of vortex shedding along the Y-axis. The second reason is related to the optimization criteria, which depended on one attack angle of wind load ( $90^\circ$ ) during the optimization phase. Furthermore, the control force tracing approach, where the force was applied to the structure in active force scheme. That means, although the FLC can implicitly overcome the probability of the destabilization state of the active force scheme, the action of passive-off control force cannot be avoided, which may cause an increase in the response under relatively small excitation forces. Fig. 26 shows a real-time control force under different wind load attack angles.

Considering the response in X-direction, a reduction of 9.9%, 12%, 4.8%, 11.6%, 15.8%, 14.1%, 7.4%, and 11.3% of uncontrolled displacement is obtained for wind attack angles of  $0^\circ, 30^\circ, 40^\circ, 50^\circ, 60^\circ, 70^\circ, 80^\circ$ , and  $90^\circ$  respectively.

Approximately the same reduction percentage in acceleration response is shown with 10.1%, 12%, 4.9%, 11.5%, 15.9%, 14.0%, 7.4%, and 11.1% of uncontrolled acceleration under wind load attack angles of  $0^\circ, 30^\circ, 40^\circ, 50^\circ, 60^\circ, 70^\circ, 80^\circ$ , and  $90^\circ$ , respectively.

As one of the comfort criteria utilized recently in ATC Guide 3 to assess the design of wind excited structures, rotational velocity is also not exceeded the specified threshold, Table 13.

A deduction can be drawn from the above discussion that the developed FLMVOC algorithm is capable not only of controlling the response of the structure for both displacement and acceleration but is also capable of adaptively withstanding the interacted action of simultaneously applied excitation on full degree of freedom structure, which stands as one of the research problems.

Moreover, applying a decentralized control system concept enables FLMVOC to adaptively manage the control system's resources even if the optimum number and capacity of the MR dampers are not obtained. This performance can be seen when relatively small values of external forces are exerted on one building side rather than the other; for example, small control forces along X-axis (across wind) have been generated by the control system under the effect of ( $90^\circ$ ) wind attack angle. Meanwhile, the structural response along Y-axis (along wind) has been controlled by maximum influential control forces.

## 4. Conclusion

The aim of this study is to develop FLMVOC, a new algorithm for adaptive vibration control systems using fuzzy logic and multiverse

optimization techniques, for building structures furnished with semi-active damper devices. For this purpose, a fuzzy logic inference system is developed and integrated with a multi-objective multiverse optimization algorithm. The analytical model for Magnetorheological Damper (MR Damper) is formulated and verified before being integrated into the FLMVOC system.

FLMVOC is applied to a three-story shear building subjected to real earthquakes with different magnitudes, demonstrating an average reduction of story drift and story acceleration about 51% and 22%, respectively. The developed system is also examined under the effect of multi-dimensional wind load with different attack angles, controlling the structure within allowable limits of movement and resident comfort criteria. The proposed optimal controller efficiently reduced both acceleration and displacement response in the range of 12% to 16% under the effect of multi-directional wind load, without amplifying either.

The result of this study proved that the proposed FLMVOC system exhibited a very promising and competitive model-free (data-driven) control strategy that can be used to control the structural response with uncertainties in both structural and excitation properties. Furthermore, FLMVOC demonstrated exceptional power-saving capabilities by utilizing approximately 2 V of the MR damper's 2.5 V capacity, effectively avoiding the damper's saturation state. However, it is important to note that the optimal controller depends on the type of load pattern utilized during the offline optimization process. Further study to develop an online optimization technique is recommended.

#### Declaration of Competing Interest

The authors declare that they have no known competing financial interests or personal relationships that could have appeared to influence the work reported in this paper.

#### References

- Adeli H, Kim H. Wavelet-Hybrid Feedback-Least Mean Square Algorithm for Robust Control of Structures. *J Struct Eng* 2004;130(1):128–37. [https://doi.org/10.1061/\(asce\)0733-9445\(2004\)130:1\(128\)](https://doi.org/10.1061/(asce)0733-9445(2004)130:1(128)).
- Ahlatat AS, Ramaswamy A. Multiobjective Optimal Fuzzy Logic Control System for Response Control of Wind-Excited Tall Buildings. *J Eng Mech* 2004;130(4):524–30.
- Aldawod M, Samali B, Naghdy F, Kwok KCS. Active Control of along Wind Response of Tall Building Using a Fuzzy Controller. *Eng Struct* 2004;23(11):1512–22. [https://doi.org/10.1016/S0141-0296\(01\)00037-2](https://doi.org/10.1016/S0141-0296(01)00037-2).
- Aly AM. Vibration Control of Buildings Using Magnetorheological Damper: A New Control Algorithm. *Journal of Engineering (United Kingdom)* 2013;2013:1–10.
- Mousaad A, Zasso A, Resta F. On the Dynamics of a Very Slender Building under Winds: Response Reduction Using MR Dampers with Lever Mechanism. *Struct Design Tall Spec Build* 2011;20(5):539–51. <https://doi.org/10.1002/tal.647>.
- ASCE 07-16. 2017. *Minimum Design Loads and Associated Criteria for Buildings and Other Structures*. Reston, VA: American Society of Civil Engineers. <https://doi.org/10.1061/9780784414248>.
- ATC. 2019. 'ATC Design Guide 3 - Serviceability Design of Tall Buildings Under Wind Load'.
- B. F. Spencer Jr., and S. Nagarajaiah. 2003. 'State of the Art of Structural Engineering'. *Perspectives in Civil Engineering: Commemorating the 150th Anniversary of the American Society of Civil Engineers*, no. July: 131–41. [https://doi.org/10.1061/\(asce\)0733-9445\(2002\)128:8\(965\)](https://doi.org/10.1061/(asce)0733-9445(2002)128:8(965)).
- Bel Hadj Ali, N., and I.F.C. Smith. 2010. 'Dynamic Behavior and Vibration Control of a Tensegrity Structure'. *International Journal of Solids and Structures* 47 (9): 1285–96. <https://doi.org/10.1016/j.ijsolstr.2010.01.012>.
- Bhowmik, Subrata. 2012. 'Modelling and Control of Magnetorheological Damper: Real-Time Implementation and Experimental Verification'.
- Bianchi Santos, Rodrigo, Waldy Jair Torres Zuniga, and Anderson Pereira. 2019. 'SAP2000-MATLAB INTEGRATION FOR NONLINEAR DYNAMIC RESPONSE STRUCTURAL OPTIMIZATION'. In *Proceedings of the 25th International Congress of Mechanical Engineering*. ABCM. <https://doi.org/10.26678/ABCM.COBEM2019.COB2019-1942>.
- Vinay C, Agrawal V, Nagar R. Applications of Soft Computing in Civil Engineering: A Review. *International Journal of Computer Applications* 2013;81(10):13–20. <https://doi.org/10.5120/14047-2210>.
- Chen Y, Feng J. Generalized Eigenvalue Analysis of Symmetric Prestressed Structures Using Group Theory. *J Comput Civ Eng* 2012;26(4):488–97. [https://doi.org/10.1061/\(asce\)cp.1943-5487.0000151](https://doi.org/10.1061/(asce)cp.1943-5487.0000151).
- Christodoulou, Manolis, Yiannis Boutalis, and Dimitrios Theodoridis. 2009. 'Indirect Adaptive Control of Unknown Nonlinear Systems with Parametric and Dynamic Uncertainties: A New Neuro-Fuzzy Method, Employing a Novel Approach of Parameter Hopping'. *IFAC Proceedings Volumes (IFAC-PapersOnline)* 2 (PART 1): 79–85. <https://doi.org/10.3182/20090921-3-TR-3005.00016>.
- CSI. 2020. 'Open Application Programming Interface'. Computers and Structures incorporation. [www.csiamerica.com](http://www.csiamerica.com).
- Das D, Datta TK, Madan A. Semiactive Fuzzy Control of the Seismic Response of Building Frames with MR Dampers. *Earthq Eng Struct Dyn* 2012;41(1):99–118. <https://doi.org/10.1002/eqe.1120>.
- Duthinh, Dat, and Emil Simiu. 2011. 'The Use of Wind Tunnel Measurements in Building Design'.
- Dyke SJ, Spencer BF, Sain MK, Carlson JD. Modeling and Control of Magnetorheological Dampers for Seismic Response Reduction. *Smart Mater Struct* 1996;5(5):565–75. <https://doi.org/10.1088/0964-1726/5/5/006>.
- Dyke SJ, Spencer BF, Sain MK, Carlson JD. Seismic Response Reduction Using Magnetorheological Dampers. *IFAC Proceedings Volumes* 1996;29(1):5530–55. [https://doi.org/10.1016/S1474-6670\(17\)58562-6](https://doi.org/10.1016/S1474-6670(17)58562-6).
- Dyke, S J, Billie F Spencer Jr., M K Sain, and J D Carlson. 1996. 'Experimental Verification of Semi-Active Structural Control Strategies Using Acceleration Feedback'. *Proceedings of the 3rd International Conference on Motion and Vibration Control* 3: 291–96.
- Gutierrez Soto, Mariantonieta, and Hojjat Adeli. 2017a. 'Many-Objective Control Optimization of High-Rise Building Structures Using Replicator Dynamics and Neural Dynamics Model'. *Structural and Multidisciplinary Optimization* 56 (6): 1521–37. <https://doi.org/10.1007/s00158-017-1835-9>.
- Gutierrez Soto, Mariantonieta, and Hojjat Adeli. 2017b. 'Multi-Agent Replicator Controller for Sustainable Vibration Control of Smart Structures'. *Journal of Vibroengineering* 19 (6): 4300–4322. <https://doi.org/10.21595/jve.2017.18924>.
- Housner GW, Bergman LA, Caughey TK, Chassiakis AG, Claus RO, Masri SF, et al. Structural Control: Past, Present, and Future. *J Eng Mech* 1997;123(9):897–971. [https://doi.org/10.1061/\(asce\)0733-9399\(1997\)123:9\(897\)](https://doi.org/10.1061/(asce)0733-9399(1997)123:9(897)).
- Jafari M, Alipour A. Methodologies to mitigate wind-induced vibration of tall buildings: A state-of-the-art review. *Journal of Building Engineering* 2021;33:101582.
- Jiang, Xiaomo, and Hojjat Adeli. 2008a. 'Dynamic Fuzzy Wavelet Neuroemulator for Non-Linear Control of Irregular Building Structures'. *International Journal For Numerical Methods In Engineering Int*. 74 (Decemer): 1045–66. <https://doi.org/10.1002/nme>.
- Jiang, Xiaomo, and Hojjat Adeli. 2008b. 'Neuro-Genetic Algorithm for Non-Linear Active Control of Structures'. *International Journal For Numerical Methods In Engineering Int*. 75 (February): 770–86. <https://doi.org/10.1002/nme>.
- Joghataie, Abdolreza, and Mohtasham Mohebbi. 2012. 'Optimal Control of Nonlinear Frames by Newmark and Distributed Genetic Algorithms'. *The Structural Design of Tall and Special Buildings* 21 (July 2014): 77–95. <https://doi.org/10.1002/tal>.
- Kaveh, A, and Omid Khademhosseini. 2015. 'Semi-Active Tuned Mass Damper Performance with Optimized Fuzzy Controller Using CSS Algorithm', no. January.
- Khaje-Karamodin A, Haji-Kazemi H, Rowhanimanesh AR, Akbarzadeh-Tootoonchi MR. Semi-Active Control of Structures Using a Neuro-Inverse Model of MR Dampers. *Sci Iran* 2009;16(3):256–63.
- Khazaei, Mohsen, Reza Vahdani, and Ali Kheyroddin. 2020. 'Optimal Location of Multiple Tuned Mass Dampers in Regular and Irregular Tall Steel Buildings Plan'. *Shock and Vibration, Hindawi* 2020: 20. <https://doi.org/doi.org/10.1155/2020/9072637> Research.
- Li, Luyu, and Haizhi Liang. 2018. 'Semiactive Control of Structural Nonlinear Vibration Considering the MR Damper Model'. *Journal of Aerospace Engineering* 31 (6): 04018095. [https://doi.org/10.1061/\(asce\)as.1943-5525.0000902](https://doi.org/10.1061/(asce)as.1943-5525.0000902).
- Li Z, Adeli H. Control Methodologies for Vibration Control of Smart Civil and Mechanical Structures. *Expert Syst* 2018;35(6):1–20. <https://doi.org/10.1111/exsy.12354>.
- MATLAB SIMULINK. 2016. 'Dynamic System Simulation for Matlab'. Natick, Massachusetts: Mathworks Inc.
- Mirjalili S, Jangir P, Mirjalili SZ, Saremi S, Trivedi IN. Optimization of Problems with Multiple Objectives Using the Multi-Vers Optimization Algorithm. *Knowledge-Based Syst* 2017;134:50–71. <https://doi.org/10.1016/j.knsys.2017.07.018>.
- Mirjalili S, Mirjalili SM, Hatamlou A. Multi-Vers Optimizer: A Nature-Inspired Algorithm for Global Optimization. *Neural Comput & Applic* 2016;27(2):495–513. <https://doi.org/10.1007/s00521-015-1870-7>.
- Park, Sejun. 2018. 'NIST Technical Note 2001 Introductory Tutorial for DAD : Design Examples of High-Rise Building for Wind NIST Technical Note 2001 Introductory Tutorial for DAD : Design Examples of High-Rise Building for Wind'. In *NIST BUILDING SCIENCE SERIES 181*.
- Peng GR, Li WH, Du H, Deng HX, Alici G. Modelling and Identifying the Parameters of a Magneto-Rheological Damper with a Force-Lag Phenomenon. *App Math Model* 2014;38(15–16):3763–73. <https://doi.org/10.1016/j.apm.2013.12.006>.
- Peng Y, Zhang Z. Optimal MR Damper-Based Semiactive Control Scheme for Strengthening Seismic Capacity and Structural Reliability. *J Eng Mech* 2020;146(6):04020045. [https://doi.org/10.1061/\(asce\)em.1943-7889.0001768](https://doi.org/10.1061/(asce)em.1943-7889.0001768).
- Pourzeynali S, Lavasani HH, Modarayi AH. Active Control of High Rise Building Structures Using Fuzzy Logic and Genetic Algorithms. *Eng Struct* 2007;29(3):346–57. <https://doi.org/10.1016/j.engstruct.2006.04.015>.
- Ross, Timothy J. 2010. *Fuzzy Logic With Engineering*. Third Edit.
- Singh, M P, and Shih-Chi Liu. 2008. "Structural Control, Advanced Sensing Systems and Health Monitoring: Past, Present and Future". *14th World Conference on Earthquake Engineering (14WCEE)*.
- Soong TT, Spencer BF. Active, Semi-Active and Hybrid Control of Structures. *Bull NZ Soc Earthq Eng* 2000;33(3):387–402. <https://doi.org/10.5459/bnzsee.33.3.387-402>.

- [43] Spence, Seymour M J. 2009. 'High-Rise Database-Assisted Design 1.1 (HR\_DAD\_1.1): Concepts, Software, and Examples'. In *NIST BUILDING SCIENCE SERIES 181*. Vol. 1.
- [44] Spencer BF, Dyke SJ, Sain MK, Carlson JD. Phenomenological Model for Magnetorheological Dampers. *J Eng Mech* 1997;123(3):230–328. [https://doi.org/10.1061/\(asce\)0733-9399\(1997\)123:3\(230\)](https://doi.org/10.1061/(asce)0733-9399(1997)123:3(230)).
- [45] Utku S. Incorporating Intelligence into Engineered Products: Adaptive Structures. *Int J Comput Appl Technol* 2000;13(1):1–9. <https://doi.org/10.1504/ijcat.2000.000219>.
- [46] Wang DH, Liao WH. Magnetorheological Fluid Dampers: A Review of Parametric Modelling. *Smart Mater Struct* 2011;20(2):023001.
- [47] Wang, Nengmou. 2011. 'Modified Sliding Mode Control Algorithm for Vibration Control of Linear and Nonlinear Civil Structures'.
- [48] Wang N, Adeli H. Self-Constructing Wavelet Neural Network Algorithm for Nonlinear Control of Large Structures. *Eng Appl Artif Intel* 2015;41(May):249–58. <https://doi.org/10.1016/j.engappai.2015.01.018>.
- [49] Xu K, Dai Q, Bi K, Fang G, Ge Y. Closed-form Design Formulas of TMDI for Suppressing Vortex-induced Vibration of Bridge Structures. *Struct Control Health Monit* 2022;29(10). <https://doi.org/10.1002/stc.3016>.
- [50] Zafarani MM, Halabian AM. A New Supervisory Adaptive Strategy for the Control of Hysteretic Multi-Story Irregular Buildings Equipped with MR-Dampers. *Eng Struct* 2020;217(August):110786. <https://doi.org/10.1016/j.engstruct.2020.110786>.
- [51] Zhang W, Ning J, Zhang M, Pei Y, Liu B, Sun Bo. Multiresolution Streamline Placement Based on Control Grids. *Integr Comput-Aided Eng* 2014;21(1):47–57.
- [52] Zhang P, Fan W, Chen Y, Feng J, Sareh P. Structural symmetry recognition in planar structures using Convolutional Neural Networks. *Eng Struct* 2022;260:114227.
- [53] Hu X, Fang G, Yang J, Zhao L, Ge Y. Simplified models for uncertainty quantification of extreme events using Monte Carlo technique. *Reliab Eng Syst Saf* 2023;230:108935.
- [54] Steffen S, Zeller A, Böhm M, Sawodny O, Blandini L, Sobek W. Actuation concepts for adaptive high-rise structures subjected to static wind loading. *Eng Struct* 2022;267:114670.
- [55] Xu K, Chen L, Lopes AM, Wang M, Li X. Adaptive fuzzy variable fractional-order sliding mode vibration control of uncertain building structures. *Eng Struct* 2023;282:115772.
- [56] Zhang Y, Schauer T, Bleicher A. Optimized Passive/Semi-Active Vibration Control Using Distributed-Multiple Tuned Facade Damping System in Tall Buildings. *Journal of Building Engineering* 2022;52(July):104416. <https://doi.org/10.1016/j.jobe.2022.104416>.
- [57] Zhou Li, Chang C-C, Wang L-X. Adaptive Fuzzy Control for Nonlinear Building-Magnetorheological Damper System. *J Struct Eng* 2003;129(7):905–13. [https://doi.org/10.1061/\(asce\)0733-9445\(2003\)129:7\(905\)](https://doi.org/10.1061/(asce)0733-9445(2003)129:7(905)).